DOI: 10.1002/ejoc.200900236

Molecular Designs and Syntheses of Organic Dyes for Dye-Sensitized Solar Cells

Yousuke Ooyama*[a] and Yutaka Harima*[a]

Keywords: Dye-sensitized solar cells / Dyes/pigments / Energy conversion / Photochemistry / Photosensitizers / Photovoltaic performances

Dye-sensitized solar cells (DSSCs) based on organic dyes adsorbed on nanocrystalline TiO_2 electrodes have received considerable attention because of their high incident solar light-to-electricity conversion efficiency and low cost of production. A number of organic dyes have so far been developed, and the relationship between their chemical structures and the photovoltaic performances of DSSCs based on the dyes has been examined. To create high-performance DSSCs, it is important to develop effective organic dye sensitizers, which should be optimized for the chemical structures to possess good light-harvesting features, to provide good electron communication between the dyes and a TiO_2 electrode, and to control the molecular arrangements on the TiO_2 electrode. The aim of this microreview is to highlight the design and synthesis of organic dyes for DSSCs based on recent work of organic chemists.

1. Introduction

The ever increasing consumption of fossil fuels, causing global warming and environmental pollution, has led to a greater focus on renewable energy sources and sustainable development. Among several new energy technologies, solar cells utilizing the sun as an energy source are the most promising. Traditional solar cells based on silicon have reasonable energy conversion efficiencies of ca. 15%.[1] However, they require high-purity silicon and skilled manufacturing techniques, which result in high costs, so their widespread use in our lives has been limited.

On the other hand, dye-sensitized solar cells (DSSCs) based on dye sensitizers adsorbed on nanocrystalline TiO_2

[a] Department of Applied Chemistry, Graduate School of Engineering
Hiroshima University
Higashi-Hiroshima 739-8527, Japan
Fax: +81-82-424-5494
E-mail: yooyama@hiroshima-u.ac.jp
harima@mls.ias.hiroshima-u.ac.jp

Yousuke Ooyama was born in 1977 in Kagawa, Japan, and received his B.Sc. from the Faculty of Science, Kochi University in 1999 and his M.Sc. from the Graduate School of Science, Kochi University in 2001. After his M.Sc., he joined Sanyo Chemical Industries Ltd., in 2001. After this he studied and received his Ph.D. from the Graduate School of Science, Kochi University in 2005 under the direction of Professor Katsuhira Yoshida, on a thesis entitled "Solid-state Photophysical Properties and Functional Material Characteristics of Novel Heterocyclic Quinol-type Fluorophores". He was a research fellow of the Japan Society for the Promotion of Science (JSPS) from 2003–2004. After his doctoral degree, he was appointed as an Assistant Professor at the Graduate School of Engineering, Hiroshima University, in 2005. He was a Visiting Researcher with Professor Lothar Dunsch at the Leibniz Institute for Solid State and Materials Research Dresden (IFW Dresden) in 2007. His current research interests include the design and synthesis of solid-state fluorescent dyes and dye sensitizers for Dye-Sensitized Solar Cells (DSSCs).

Prof. Yutaka Harima received his B.Eng. (1975) from the Tokyo Institute of Technology (TIT), and his M.Eng. (1977) and D.Sc. (1980) degrees from the Graduate School of TIT under the supervision of Prof. Shigeru Aoyagui. He joined the Faculty of Integrated Arts and Sciences, Hiroshima University, in 1982. He worked with Prof. S.R. Morrison at Simon Fraser University, Canada, (1985–1987). He moved to the Graduate School of Engineering, Hiroshima University, in 2002. His research activities include 1) a novel technique to evaluate electron-transfer rates of electrode reactions, 2) electrode kinetics of solvated electrons, 3) electronic properties of molecular thin films and their application to organic solar cells, 4) a novel technique to form unrestricted patterns of organic thin films, 5) electrochemiluminescence of a Ru complex and its application to a trace analysis, 6) gas sensor work based on new principles, 7) photophysical study of novel functionality molecules, 8) charge-transport mechanisms in π-conjugated polymers, 9) development of organic light-emitting diodes, 10) synthesis and photophysics of novel solid-state fluorophores, 11) fabrication of microspheres based on conducting polymers, 12) electromodulation spectroscopy for detecting charge-carrying species in organic thin films, 13) trapping of atomic hydrogen in molecular capsules, and 14) ESR study of oxygen species on TiO_2. He has published over 160 papers in the diverse research fields of science and technology.

electrodes have received considerable attention because of their high incident solar light-to-electricity conversion efficiency, colourful and decorative natures and low cost of production[2–15] since Grätzel and co-workers reported good solar cell performances for DSSCs based on a Ru complex dye in 1991.[16] The most efficient Ru-sensitizers are *cis*-dithiocyanobis(4,4′-dicarboxy-2,2′-bipyridine)ruthenium(II) {[Ru(dcbpy)$_2$(NCS)$_2$], **N3**, Figure 1}[17] and trithiocyanato-4,4′,4′′-tricarboxy-2,2′:6′,2′′-terpyridineruthenium(II) {[Ru(tcterpy)(NCS)$_3$], **black dye**},[18] owing to their intense and wide-range absorption of visible light. Under standard air mass (AM) 1.5 simulated sunlight (100 mW cm^{-2}), an **N3** dye-sensitized solar cell gave a power conversion efficiency (η) of up to 10% with a short-circuit photocurrent density (J_{sc}) of 18.2 mA cm^{-2}, an open-circuit photovoltage (V_{oc}) of 720 mV and a fill factor (*ff*) of 0.73. The incident photon-to-current conversion efficiency (IPCE) is over 80% in the visible region.

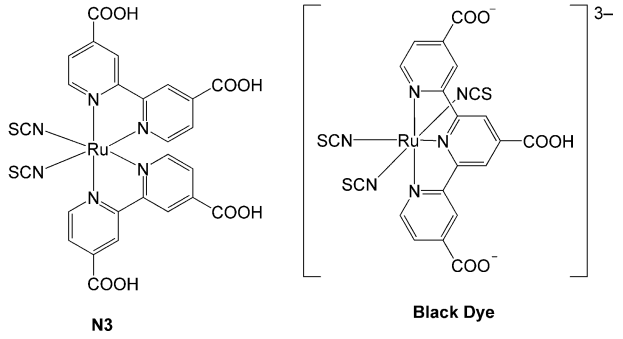

Figure 1. Examples of Ru-polypyridyl complexes used as photosensitizers for DSSCs.

As well as Ru-sensitizers, organic dyes have recently been stimulating intensive research efforts because of their advantages as photosensitizers for DSSCs: 1) they can be prepared and purified easily at lower cost, 2) they have higher molar absorption coefficients than the Ru complexes, so organic dyes have efficient light-harvesting capabilities over the wide spectral region of sunlight, 3) the wide variety of the structures and their facile modification provides potential for molecular design, with the introduction of substituents onto the chromophore skeletons allowing for easy control not only of their photophysical and electrochemical properties but also of their stereochemical structures, and 4) there are no concerns about resource limitations, because organic dyes do not contain rare metals such as ruthenium and platinum. Many organic dyes exhibiting relatively high DSSC performances have so far been designed and developed. They include coumarin dyes,[19–23] polyene dyes,[24–32] hemicyanine dyes,[33–37] thiophene-based dyes,[38–47] indoline dyes,[48,49] heteropolycyclic dyes,[50–52] xanthene dyes,[53–57] perylene dyes,[58–62] porphyrin dyes,[63–76] merocyanine dyes,[77,78] catechol dyes,[79–81] polymeric dyes,[82–88] squaraine dyes,[89–94] cyanine dyes[95–98] and phthalocyanine dyes.[99–105] Under standard air mass (AM) 1.5 simulated sunlight (100 mW cm^{-2}), the DSSC based on indoline dye **D205** (Figure 2) has shown a power conversion efficiency (η) of up to 9.5%, with a short-circuit photocurrent density (J_{sc}) of 18.7 mA cm^{-2}, an open-circuit photovoltage (V_{oc}) of 710 mV and a fill factor (*ff*) of 0.71. The incident photon-to-current conversion efficiency (IPCE) in the visible is over 80%.[49] The performances of organic-dye-based DSSCs remain inferior to those of DSSCs based on the Ru complexes, however, because of some disadvantages as photosensitizers: 1) they have relatively narrow absorption bands in the visible, which cause poorer light-harvesting in sunlight, 2) they are liable to enter into π-stacked aggregation on the TiO_2 surface, which leads to reductions in the yields of electron injection from the dyes to the conduction band (CB) of TiO_2, owing to intermolecular energy transfer, and 3) the stabilities of organic dyes are generally lower than those of Ru complexes, which may be attributable to the formation of unstable radicals under strong light irradiation.[43,78] Therefore, to overcome the above disadvantages as photosensitizers for DSSCs, it is necessary to design and synthesize new and efficient organic photosensitizers with effective chromophores and substituents for the performance of DSSCs, to be made possible by exquisite molecular designs and synthetic strategies developed by organic chemists.

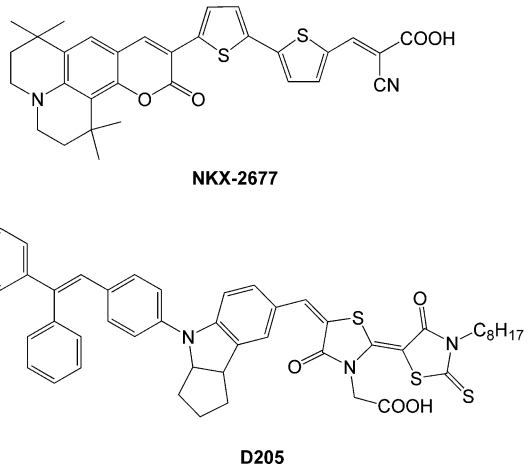

Figure 2. Examples of organic dyes used as photosensitizers for DSSCs.

2. Operational Principle of DSSCs

A schematic representation of the construction and the operational principle of a typical DSSC is shown in Figure 3. The DSSC is composed of a photo-anode and a photoinert counter electrode (cathode) sandwiching a redox mediator. It consists of five materials: 1) a fluorine-doped SnO_2 (FTO) glass substrate, 2) a nanocrystalline TiO_2 thin film as a semiconductor, 3) a dye sensitizer, 4) an electrolyte (redox mediator), and 5) a platinum-coated glass substrate. The photo-anode is made of the dye-adsorbed TiO_2 electrode; a nanocrystalline TiO_2 was applied onto the FTO glass substrate and the obtained 5–10 μm thick TiO_2 substrate was then immersed into a solution of dye for a period sufficient for the dye to adsorb on the TiO_2 surface. The

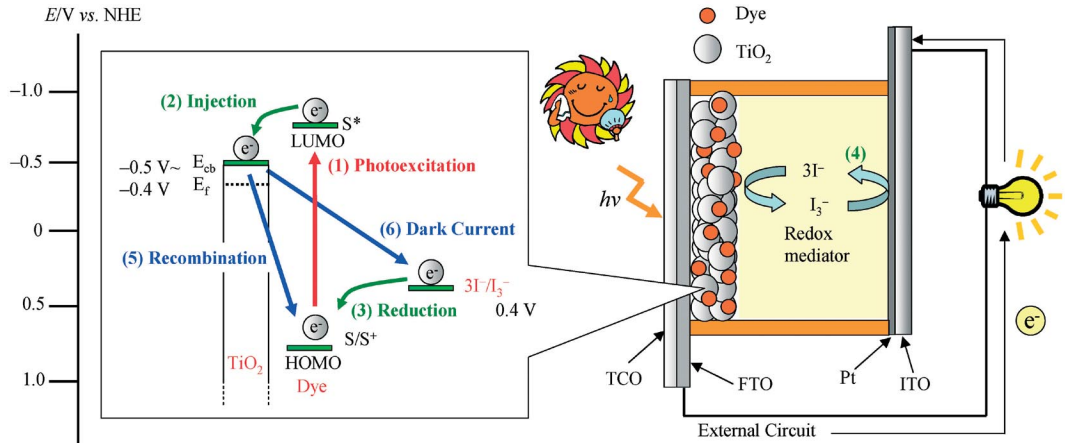

Figure 3. A schematic representation of the construction and the operational principle of DSSCs.

redox mediator is a solution containing an I_3^-/I^- couple. The Pt-coated glass plate serves as the photoinert cathode.

The generation of photocurrents in the DSSC occurs through the following processes [Equations (1) to (4)].[2–4,6–8,15,16] To begin with, the dye sensitizer absorbs a photon (sunlight) to generate the photoexcited state of the dye (S*) [Equation (1)]. Next, the photoexcited dye (S*) injects an electron into the conduction band (CB, –0.5 V vs. NHE) of TiO_2 [Equation (2)]. The resultant oxidized dye is subsequently reduced back to its original neutral state by electron donation from the I^- ions in redox mediator; this process is usually called dye regeneration or rereduction [Equation (3)]. The injected electrons move through the network of interconnected TiO_2 nanoparticles to arrive at the transparent conducting oxide (FTO) and then through the external circuit to the counter electrode (Pt-coated glass). The I^- ion is regenerated by the reduction of triiodide ion I_3^- at the counter electrode through the donation of electrons from the external circuit [Equation (4)] and then the circuit is completed. During this electron flow cycle, however, there are undesirable side processes: the electrons injected into the CB of the TiO_2 electrode may recombine either with oxidized dye [recombination, Equation (5)], or with I_3^- at the TiO_2 surface [dark current, Equation (6)], resulting in lowering of the photovoltaic performances of DSSCs. The recombination process [Equation (5)] is almost always in competition with the rereduction of the oxidized dyes by I^- [Equation (3)]. Consequently, the processes of electron injection and regeneration [Equations (2) and (3)] must be kinetically more favourable than those of the recombination and dark current [Equations (5) and (6)] in order to generate greater photocurrents and photovoltages.

$$S\ (\text{on } TiO_2) + h\nu \rightarrow S^* \quad (1)$$

$$S^*\ (\text{on } TiO_2) \rightarrow S^+\ (\text{on } TiO_2) + e^-\ (TiO_2) \quad (2)$$

$$2S^+\ (\text{on } TiO_2) + 3I^- \rightarrow 2S\ (\text{on } TiO_2) + I_3^- \quad (3)$$

$$I_3^- + 2e^-\ (Pt) \rightarrow 3I^- \quad (4)$$

$$S^+\ (\text{on } TiO_2) + e^-\ (TiO_2) \rightarrow S\ (\text{on } TiO_2) \quad (5)$$

$$I_3^- + 2e^-\ (TiO_2) \rightarrow 3I^- \quad (6)$$

2.1. Photovoltaic Parameters that Characterize the Performances of DSSCs

The performances of DSSCs are characterized mainly by six parameters: incident photon-to-current conversion efficiency (IPCE), photocurrent/voltage curve (J/V curve), open-circuit voltage (V_{oc}), short-circuit photocurrent density (J_{sc}), fill factor (ff), and solar energy-to-electricity conversion yield (η). These photovoltaic parameters are explained below.

2.1.1. Incident Photon-to-Current Conversion Efficiency (IPCE)

The IPCE is defined as the number of electrons flowing through the external circuit divided by the number of incident photons and can be represented by Equation (7).

$$\text{IPCE}\ (\%) = \frac{1240\ (\text{eV nm})\ J_{ph}\ (\text{mA cm}^{-2})}{\lambda\ (\text{nm})\ I\ (\text{mW cm}^{-2})} \quad (7)$$

where J_{ph} is the short-circuit photocurrent density generated by monochromatic light, and λ and I are the wavelength and the intensity of the monochromatic light, respectively. A plot of IPCE versus excitation wavelength is termed an IPCE spectrum or a photocurrent action spectrum. The IPCE spectrum is very useful for the evaluation of a new dye sensitizer for DSSCs. A typical IPCE spectrum is shown in Figure 4.

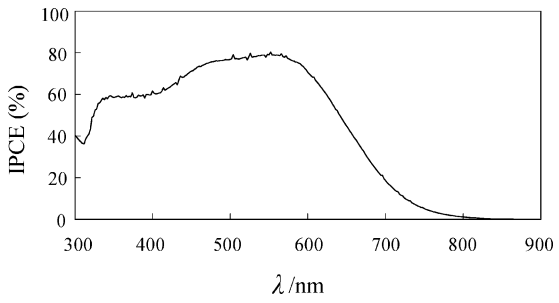

Figure 4. Typical IPCE spectrum of DSSC.

On the other hand, IPCE can also be expressed as the product of light harvesting efficiency [LHE(λ)] for photons of wavelength λ, the quantum yield of electron injection (Φ_{inj}) from the excited dye sensitizer to the conduction band of the TiO_2 electrode, and the efficiency of collection of the injected electron (Φ_{coll}) at the FTO glass [Equation (8)].

$$IPCE(\lambda) = LHE(\lambda)\Phi_{inj}\Phi_{coll} \quad (8)$$

IPCE is therefore directly related to the absorption properties of the dye, the amount of adsorbed dyes on the TiO_2 surface (or LHE), the quantum yield of electron injection from the excited dye to the CB of the TiO_2, and the efficiency of collection of electrons in the external circuit. The maximum IPCEs for DSSCs lie in the 80–85% range; they do not reach 100% experimentally because of reflection and absorption losses (10–15%) due to the FTO glass.

2.1.2. Photocurrent/Voltage Curve (*J*/*V* curve)

Measurement of the *J*/*V* curve is an easy and useful method for the evaluation of the photovoltaic performance of a DSSC. A typical *J*/*V* curve is depicted in Figure 5. The performances of DSSCs are universally represented by the following four key factors: 1) open-circuit photovoltage (V_{oc}), 2) short-circuit photocurrent density (J_{sc}), 3) fill factor (*ff*), and 4) solar energy-to-electricity conversion yield (η).

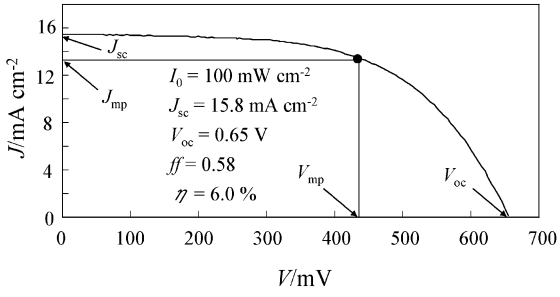

Figure 5. Typical *J*/*V* curve of a DSSC.

(1) Open-Circuit Photovoltage (V_{oc})

The V_{oc} is the difference in electrical potential between two terminals of a cell under illumination when the circuit is open (no current flow). The maximum V_{oc} of a DSSC corresponds to the difference between the energy level of the CB [exactly the Fermi level (E_f); –0.5 to –0.4 V vs. NHE] of TiO_2 and the redox potential (0.4 V vs. NHE) of the electrolyte (I_3^-/I^-): generally 0.8 to 0.9 V. However, the actual V_{oc} is lower than the theoretical value because of the recombination of injected electrons with dye cations [recombination, Equation (5)] and with I_3^- ions in the electrolyte [Equation (6), dark current]. In particular, the dark current is a primary factor leading to lower V_{oc}. On the other hand, the shift of the CB level of TiO_2 is dependent on the molecular dipole at the dye/TiO_2 interface. A shift of the CB towards the vacuum level (i.e., a negative shift of the Fermi level of TiO_2) by the increased dipole at the dye/TiO_2 interface results in a higher V_{oc}. Therefore, the V_{oc} value is strongly dependent both on the dark current and on the Fermi level of TiO_2. To obtain high V_{oc} values for DSSCs, 4-*tert*-butylpyridine (TBP) is generally added to the electrolyte: TBP adsorbed on the TiO_2 surface induces a negative shift of the CB level of TiO_2 and suppression of charge recombination (dark current) between injected electrons and I_3^- ions on the TiO_2 surface, resulting in an improved V_{oc} value.

(2) Short-Circuit Photocurrent Density (J_{sc})

J_{sc} is the photocurrent per unit area (mA cm^{-2}) when a DSSC under irradiation is short-circuited. V_{oc} corresponds to the difference between the Fermi level (E_f) of the electron in TiO_2 and the redox potential of the electrolyte (I_3^-/I^-), whereas J_{sc} is related to the interaction between TiO_2 and the dye sensitizer, as well as the absorption coefficient of the dye sensitizer. A high J_{sc} value is thus associated with the following characteristics: 1) intense light absorption capabilities of dyes over the wide region of sunlight, 2) high electron injection efficiencies from photoexcited dyes to the CB of the TiO_2 [Equation (2)], efficient rereduction of the oxidized dye by I^- [Equation (3)]. The enhancement of electron injection related to higher J_{sc} results in higher IPCEs. J_{sc} strongly depends on the photophysical and electrochemical properties of the dye sensitizers. To obtain new and efficient organic sensitizers for DSSCs, novel molecular designs not only featuring intense sunlight-harvesting properties, but also capable of strong interactions between dye sensitizers and TiO_2 surfaces are necessary.

(3) Fill Factor (*ff*)

The *ff* of a solar cell is defined as the maximum power output ($J_{mp}V_{mp}$) divided by the product of J_{sc} and V_{oc}, and is also an important parameter for DSSCs [Equation (9)].

$$ff = (J_{mp}V_{mp})/(J_{sc}V_{oc}) \quad (9)$$

The *ff* is determined from the *J*/*V* curve and is an indication of how much of the area of the rectangle for $J_{sc}V_{oc}$ is filled by that described by $J_{mp}V_{mp}$ (Figure 5).

(4) Solar Energy-to-Electricity Conversion Yield (η)

The η value of a DSSC is defined as the ratio of the maximum output electrical power of the DSSC to the energy of incident sunlight (I_0). The η value is therefore determined [Equation (10)] by V_{oc}, J_{sc}, *ff* and I_0 (generally 100 mW cm^{-2}).

$$\eta\,(\%) = \frac{J_{sc}\,(\text{mA cm}^{-2})\;V_{oc}\,(\text{V})\;ff}{I_0\,(\text{mW cm}^{-2})} \quad (10)$$

Consequently, to obtain a high η value, optimization of the values of J_{sc} and V_{oc} of the cell is essential. To date, η values have been improved gradually through molecular design of dye sensitizers. The design and synthesis of more efficient organic dyes for DSSCs, in which the interactions between neighboring dyes on the TiO_2 surface, between dye and TiO_2, between dye and electrolyte, and between TiO_2 and electrolyte are considered, as well as the photoabsorption abilities of the dye sensitizer, remain necessary.

3. Molecular Design of Organic Dyes for DSSCs

On the basis of the accumulated knowledge of organic dyes so far synthesized for DSSCs, the indispensable requirements in the molecular design of organic dyes for DSSCs are as follows:[20,31,40]

1) The organic dye must have at least one anchoring group (e.g., –COOH, $–SO_3H$, $–PO_3H_2$, –OH) for adsorption onto the TiO_2 surface. In particular, a carboxy group can form an ester linkage with the TiO_2 surface to provide a strongly bound dye and good electron communication between them.

2) To achieve efficient electron injection from the excited dye to the CB of the TiO_2, the energy level of the lowest unoccupied molecular orbital (LUMO) of the dye must be higher (more negative) than the conduction band (CB) of the TiO_2 electrode. On the other hand, to achieve efficient regeneration of the oxidized state by electron transfer from I_3^-/I^- redox couple in the electrolyte, the energy level of the highest occupied molecular orbital (HOMO) of the dye must be lower (more positive) than the I_3^-/I^- redox potential (Figure 3).

3) To give high light-harvesting efficiency, the organic dye must have high molar absorption coefficients over the wide region of sunlight, to provide a large photocurrent.

4) To achieve a durable DSSC, the organic dye must have chemical stability in its photoexcited state and in the redox reactions throughout the reaction cycle.

5) Dye aggregation on the TiO_2 surface, leading to low conversion efficiency of the DSSC, should be avoided. In particular, donor–acceptor π-conjugated dyes are liable to undergo π-stacked aggregation on the TiO_2 surface, which leads to reduction in electron-injection yield from the dyes to the CB of the TiO_2 owing to intermolecular energy transfer.

6) Recombination of injected electrons with the dye and dark current [Equations (5) and (6)] should be suppressed. Efficient charge separation – wide spatial separation between the moieties of positive charge density on the exited dye and the TiO_2 surface – leads to retardation of the recombination.

According to the above requirements and the several reports of organic dyes so far used in DSSCs, requirements 1)–3) should be fulfilled by photophysical and electrochemical modifications of the dye structures through the introduction of electron-donating and electron-accepting groups onto the chromophore skeleton and by expansion of π conjugation. Requirements 4)–6), on the other hand, should be fulfilled through the introduction of sterically hindered substituents (bulky groups) such as long alkyl chains and aromatic units onto the chromophore skeleton. In summary, to obtain further new and efficient organic dye sensitizers for DSSCs, novel molecular designs capable of controlling not only the photophysical and electrochemical properties of the dyes themselves but also the molecular orientation and arrangement of dyes on the TiO_2 surface – such as π-stacked aggregation of dyes and interaction between dye sensitizers and TiO_2 surface – are necessary. The next sections illustrate the many organic dyes so far developed for DSSCs.

3.1. Donor–Acceptor π-Conjugated (D-π-A) Dyes

A large number of organic dyes have been developed, and the relationships between their chemical structures and the photovoltaic performances of DSSCs based on these dyes have been examined. In particular, donor–acceptor π-conjugated (D-π-A) dyes possessing both electron-donating (D) and electron-accepting (A) groups linked by π-conjugated bridges (D-π-A structures, as shown in Figure 6), displaying broad and intense absorption spectral features, would be expected to be one of the most promising classes of organic sensitizers.[13] Most of the D-π-A dyes have dialkylamine or diphenylamine moieties as electron donors and carboxylic acid, cyanoacrylic acid or rhodanine-3-acetic acid moieties as electron acceptors, and also as anchoring groups for attachment on TiO_2 surfaces. Carboxy groups can form ester linkages with TiO_2 surfaces to provide strongly bound dyes and good electron communication.

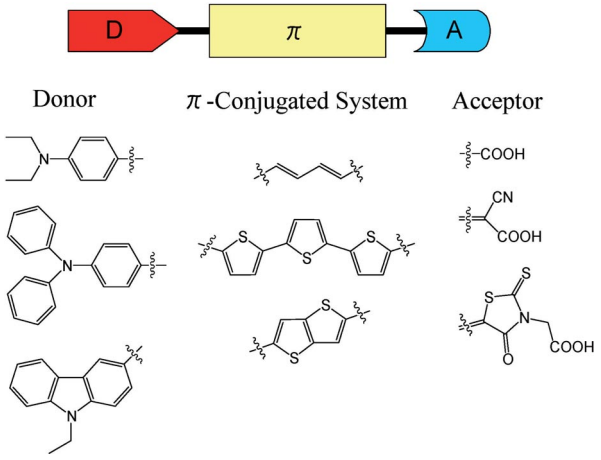

Figure 6. Schematic representation of a D-π-A organic dye sensitizer.

The photoabsorption properties of a D-π-A dye are associated with intramolecular charge transfer (ICT) excitation from the donor to the acceptor moiety of the dye, resulting in efficient electron transfer through the acceptor moiety (carboxy group) from the excited dye into the TiO_2 conduction band. The charge transfer or separation between the electron donor and acceptor moieties in the excited dye may facilitate rapid electron injection from the dye molecule into the CB of the TiO_2, so that it would be expected to separate the cationic charge effectively from the TiO_2 surface and to restrict recombination between the photoelectron (the injected electron) and the oxidized dye sensitizer efficiently. As a noteworthy structural feature of D-π-A dyes, the HOMOs of D-π-A dyes are in many cases delocalized over the π-conjugated systems in configurations centring on aminophenyl units (donor parts), while the LUMOs are delo-

calized over cyanoacrylic units (acceptor and anchor parts). The photoinduced electron transfer from D-π-A dyes to TiO_2 electrodes can thus efficiently occur by ICT with respect to HOMO-to-LUMO transition. The cations formed after the electron injection are also a good match to the redox potential of the I_3^-/I^- electrolyte. The expansion of π conjugation in the dye structures and the introduction of electron-donating and -accepting substituents into the chromophore skeletons can shift the levels of the HOMOs and LUMOs, allowing tuning of the photophysical and electrochemical properties of the dyes. In the D-π-A structure concept, increasing the electron-donating and electron-accepting abilities of donors and acceptors, respectively, decreases the energy gaps between the HOMO and LUMO, thus resulting in red-shifting of the absorption peaks. The absorption spectra of organic dyes could therefore be red-shifted by expansion of the π conjugation in the dyes and introduction of electron-donating and -accepting substituents into the dye skeletons; such substituents can shift the levels of the HOMOs and LUMOs of the dyes. Red-shifting the absorption spectra is not the only important consideration in the design of efficient organic dye photosensitizers; the potential levels of the HOMOs and LUMOs must be matched to the CB level of the TiO_2 electrode and to the redox potential of the I^-/I_3^- electrolyte.

Unfortunately, these D-π-A dyes are liable to experience π-stacked aggregation between dye molecules on TiO_2 surfaces, which tends to reduce electron-injection yields from the dyes to the CB of TiO_2, owing to intermolecular energy transfer between dyes. To prevent aggregation of dye molecules on TiO_2 surfaces, deoxycholic acid (DCA) has been generally used in a number of research works. In addition, the introduction of sterically hindered substituents (bulky groups) such as long alkyl chains and aromatic units into dye structures should efficiently suppress aggregation, due to disturbance of the π–π stacking.

In summary, the photophysical, electrochemical and related ICT properties of a D-π-A dye strongly depend on the electron-donating ability of D and the electron-accepting ability of A, as well as on the electronic characteristics of the π bridge. They should be strategically tuneable through chemical modification on each component (D, A or π bridge) to suit the requirements for efficient DSSCs. Furthermore, to prevent aggregation of dye molecules on the TiO_2 surface, the introduction of effective substituents on a suitable part of the dye skeleton is necessary. In the next subsections, the molecular designs and syntheses of some already developed D-π-A dyes for DSSCs are used to illustrate how one might hit on new ideas for designing more efficient D-π-A dye sensitizers.

3.1.1. Coumarin Dyes

Coumarin dyes are one of the most promising classes of dye sensitizers out of the D-π-A dyes so far employed for DSSCs, and have been studied systematically by Hara and Arakawa (Figure 7).[19–23] Based on the concept of the donor–acceptor π-conjugated structure, a series of new coumarin dye sensitizers possessing different numbers of thiophene and/or methine units as π-conjugation bridge between a coumarin skeleton containing an amino group as the donor component and a cyanoacrylic acid as the acceptor component have been designed and synthesized. The synthetic routes to the coumarin dye sensitizers **NKX-2311** and **NKX-2677** are shown in Scheme 1.[19,20] For the synthesis of **NKX-2311**, aldehyde **3** was prepared from **1** through a Wittig reaction[106] and a subsequent Vilsmeier–Haack reaction.[107] **NKX-2311** was then synthesized by Knoevenagel condensation[108] of the aldehyde **3** with cyanoacetic acid in the presence of piperidine. For the synthesis of **NKX-2677**, compound **7** was prepared from **6** and thiophene-2-boronic acid in the presence of $Pd(PPh_3)_4$ and K_2CO_3 (Suzuki coupling),[109] and **NKX-2677** was then synthesized in two steps by a procedure similar to that used in the case of **NKX-2311**.

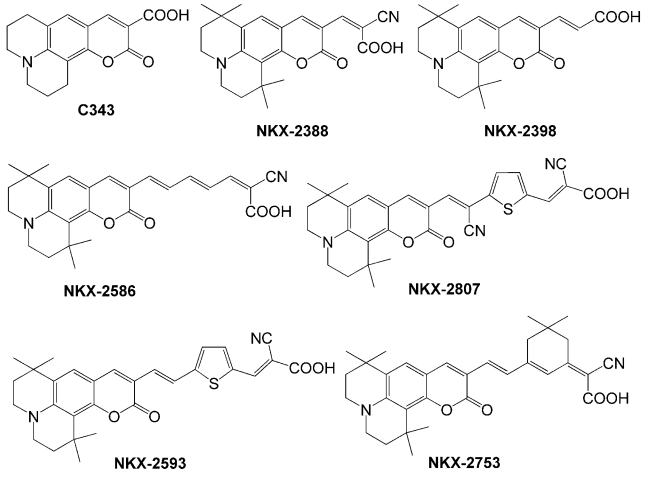

Figure 7. Molecular structures of coumarin dye sensitizers.

The absorption spectra of these new coumarin dyes are significantly red-shifted in the visible, relative to the spectrum of the typical coumarin dye **C343** (Table 1). Introduction of a methine unit (–CH=CH–) connecting both the cyano (–CN) and carboxy (–COOH) groups into the coumarin skeleton expanded the π conjugation in the dye and thus resulted in a wide absorption in the visible region:

1) The absorption maximum was gradually red-shifted by increasing the number of methine units from one to three (**NKX-2388**, **2311**, **2586**). This result suggests that the red shift in the absorption arising from the lengthening of the methine component can be attributed to negative shifts in the oxidation potentials (i.e., negative shift in the HOMOs).

2) Introducing of a cyano group shifted the reduction potential of the dye in the positive direction (i.e., a positive shift in the LUMO), because of the strong electron-accepting ability of the cyano group. This suggests that the red shift in the absorption spectrum of **NKX-2388** relative to that for **NKX-2398** is caused by a positive shift in the reduction potential.[19]

3) The introduction of one more CN group into the molecular skeleton decreases the gap between the HOMO and the LUMO. Introduction of a further cyano group into the

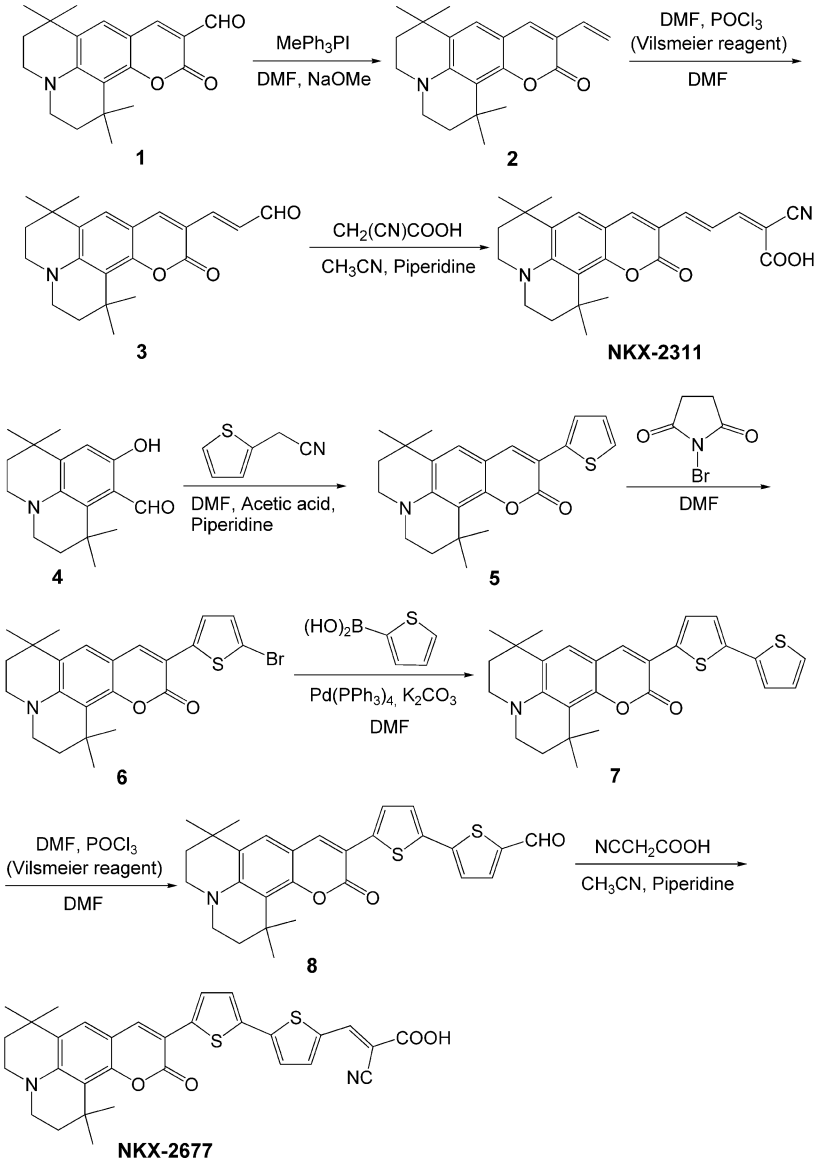

Scheme 1. Synthesis of coumarin dye sensitizers **NKX-2311** and **NKX-2677**.

Table 1. Absorption peaks of coumarin dyes and the photovoltaic performances of DSSCs based on them.

Dye	λ_{max}^{abs} [nm]	J_{sc} [mA cm^{-2}]	V_{oc} [V]	*ff*	η (%)
C343	442[a]	4.1	0.41	0.56	0.9
NKX-2311	504[a]	15.2	0.55	0.62	5.2
NKX-2388	493[a]	12.9	0.50	0.64	4.1
NKX-2398	451[a]	11.1	0.51	0.60	3.4
NKX-2586	506[a]	15.1	0.47	0.50	3.5
NKX-2593	510[b]	14.7	0.67	0.73	7.2
NKX-2677	511[c]	14.3	0.73	0.74	7.7
NKX-2753	492[b]	16.1	0.60	0.69	6.7
NKX-2807	566[b]	14.3	0.51	0.73	5.3

[a] In methanol. [b] In ethanol. [c] *t*BuOH/acetonitrile (50:50).

π conjugation bridge (**NKX-2807**)[21] positively shifts the LUMO relative to that of a dye containing one cyano group (e.g., **NKX-2593**), and thus red-shifts the maximum absorption band, allowing harvesting of more photons for photoelectric conversion in the long-wavelength region; one more electron acceptor enhances the electron-accepting ability of electron acceptors and lowers the LUMO, thus reducing the gap between HOMO and LUMO. On the other hand, in the case of **NKX-2593**, the thiophene modification of the coumarin dyes markedly improved the performance of coumarin-based DSSCs; the introduction of π-conjugated ring moieties such as thiophene into the methine backbone of **NKX-2311** simultaneously expands the π conjugation system and improves the stability of the dye molecule relative to dyes that have a long methine chain unit, although the introduction of thiophene moieties did not affect the absorption properties of the dye in solution.[20]

The photovoltaic performances of the DSSCs based on these coumarin dyes are summarized in Table 1. A DSSC based on **NKX-2677** shows an η value of 7.7% with J_{sc} of

14.3 mA cm^{-2}, V_{oc} of 730 mV and *ff* of 0.74. The IPCE is close to 80% in the visible region.

However, these coumarin dyes are liable to experience π-stacked aggregation between dye units on TiO_2 surfaces; in particular, the strong π-electron interaction in coumarin dyes containing three methine units (**NKX-2586**) leads to dye aggregation. Although π-stacked aggregation between dye units on the TiO_2 surface is advantageous to light harvesting, because of the broad feature it produces in the UV/Vis absorption spectrum, π-stacked aggregates usually lead to inefficient electron injection because of intermolecular energy transfer between the dyes, thus resulting in low power conversion efficiency and low IPCE. Deoxycholic acid (DCA) has been used to prevent aggregation of dye molecules on TiO_2 surfaces in a number of research works. Although coadsorption of coumarin dyes with DCA has proved able to prevent aggregation and hence to improve the photovoltaic performance by means of improving both photocurrent and photovoltage, the significantly decreased dye adsorption unavoidably limits the photovoltaic performance. To reduce intermolecular interaction or dye aggregation while keeping the adsorbed dye amount, the new coumarin dye **NKX-2753**, with a side ring linked to the alkene chain (Figure 7), was designed and synthesized.[22] The side ring linked to the alkene chain proved to be as effective as DCA in preventing dye aggregation. For this reason, DCA is not needed to coadsorb with **NKX-2753** on the TiO_2 surface, ensuring a high surface concentration of dye and efficient photon-to-electron conversion.

3.1.2. Polyene Dyes

Polyene dyes containing an amino moiety as the donor part and a methine (–CH=CH–) unit connecting to a cyanoacrylic acid moiety as the acceptor part, which have the simplest D-π-A molecular structures, are also one of the most promising classes of dye sensitizers and have been studied systematically by many researchers.[24–32] Extension of the methine unit induces a bathochromic shift in the absorption spectrum due to the expansion of the π conjugation system. The introduction of further amino (anilino) groups also induces bathochromic shifts in the absorption spectra, due to the increasing donation from the amino moieties. The efficient polyene dye photosensitizers **NKX-2553**, **2554** and **2569** (Figure 8) were designed and synthesized by Hara and co-workers.[24] **NKX-2553** was prepared simply through a Knoevenagel condensation between 4-dimethylaminocinnamaldehyde and cyanoacetic acid in acetonitrile in the presence of piperidine. **NKX-2554** and **NKX-2569** were synthesized from the corresponding aldehyde intermediates and cyanoacetic acid by a procedure similar to that used for **NKX-2553**. Expansion of the methine component in the aldehyde intermediate was carried out through a Vilsmeier–Haack reaction. The absorption maximum of **NKX-2553**, containing one dimethylamino moiety, is at 454 nm whereas that of **NKX-2554** (λ_{max}^{abs} = 465 nm) is slightly red-shifted through the introduction of a further dimethylamino moiety into **NKX-2553**. Moreover, after expansion of the methine unit of **NKX-2554**, the absorption spectrum of **NKX-2569** (λ_{max}^{abs} = 501 nm) is red-shifted relative to that of **NKX-2554**. These results demonstrated that the introduction of a dimethylamino moiety and expansion of the methine component contribute to red-shifting of the absorption spectra of the dyes. A DSSC based on **NKX-2569** shows an η value of 6.8% with J_{sc} of 12.9 mA cm^{-2}, V_{oc} of 710 mV and *ff* of 0.74. The onset of the IPCE spectrum reached 820 nm. The η values of **NKX-2553** and **NKX-2554** are 5.5 and 5.4%, respectively.

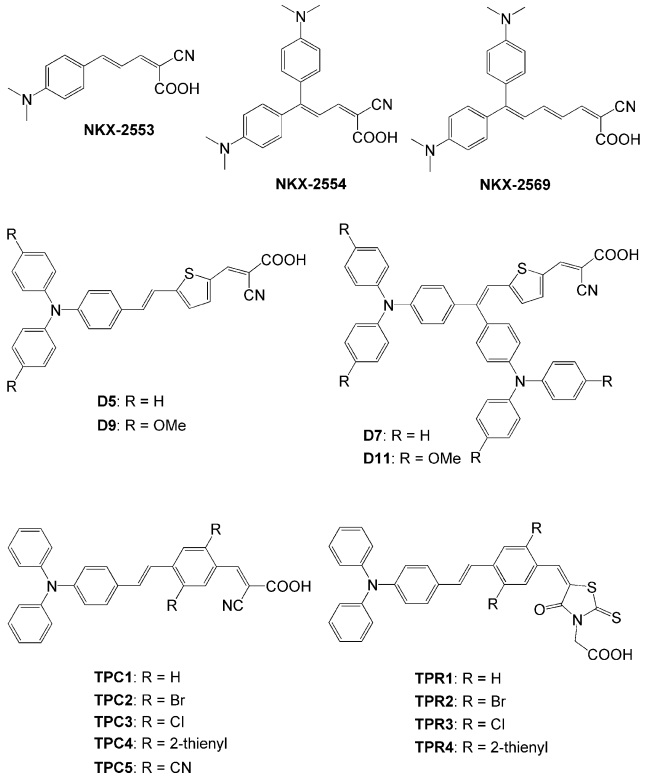

Figure 8. Molecular structures of polyene dye sensitizers **NKX**, **D**, **TPC** and **TPR**.

As mentioned above, one of the approaches to extension of the absorption regions of the dyes is to introduce a methine component in order to increase the π conjugation. However, such extended π conjugation with a methine chain often results in instability of the organic dyes, due not only to rotation, but also to *cis*/*trans* isomerization about the central methine bond (–CH=CH–). Moreover, expansion of π conjugation chains by introduction of methine units causes π-stacked aggregation through the formation of π–π interactions between dye units. A successful approach based on incorporation of a π conjugation system such as a thiophene or phenylene unit into the dye skeleton has recently been introduced; this not only increases the molar extinction coefficient of the organic sensitizer but also increases the stability. Moreover, the introduction of thiophene or phenylene units also led to broadening of the absorption spectra and gave red shifts. Sun and co-workers have systematically studied efficient DSSCs based on the polyene **D**, **TPC** and **TPR** dye classes (Figure 8), constructed with diphenylaniline moieties as both electron-donating and

bulky substituents, cyanoacrylic acid or rhodanine-3-acetic acid as both electron-accepting and anchoring groups, and thiophene or phenylene units incorporated into polyene chains.[25,26]

For the preparation of **D5**, the three-step synthesis of the dye involves well-known reactions and gives a moderate yield (Scheme 2). The thiophene moiety was coupled to 4-(diphenylamino)benzaldehyde (**9**) in a Wittig reaction, followed by formylation of the thiophene functionality and, finally, condensation of the aldehyde **11** with cyanoacetic acid in a Knoevenagel condensation in the presence of piperidine.

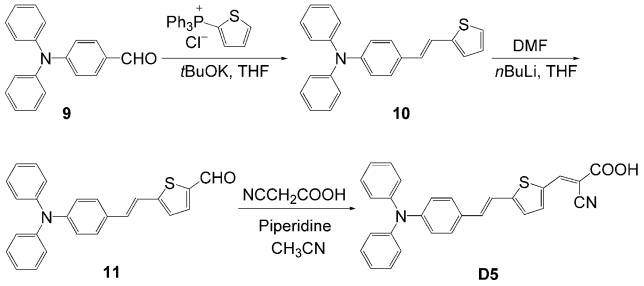

Scheme 2. Synthesis of polyene dye sensitizer **D5**.

The IPCEs of a series of D-type dyes are above 80%, and **D5**-sensitized solar cells yield J_{sc} values of 12.00 ± 0.2 mA cm^{-2}, V_{oc} values of 688 ± 10 mV, and *ff* values of 0.72 ± 0.02, corresponding to η of 5.94% under standard AM 1.5 sunlight. On the other hand, on comparison of the absorption maxima of **TPR** dyes (λ_{max}^{abs} = 464–480 nm) with those of **TPC** dyes (λ_{max}^{abs} = 438–500 nm), the introduction of rhodanine-3-acetic acid as electron acceptor contributed to the bathochromic shift of the absorption spectra because of the stronger electron-withdrawing ability of rhodanine-3-acetic acid relative to the cyanoacrylic acid unit. In general, however, **TPC** dyes show higher IPCE, J_{sc}, V_{oc} and η values than the corresponding **TPR** dyes. The *J*/*V* curves in the dark for the DSSCs based on **TPC1** and **TPR1** indicate that recombination reactions between the injected electrons in the TiO_2 and the I_3^- ion in the electrolyte occur more easily in DSSCs based on **TPR** dyes than in DSSCs based on **TP1** dyes. From density functional theory (DFT) calculations, the LUMOs of **TPC** dyes containing cyanoacrylic acid anchor groups have much better orbital overlap with the TiO_2 conduction band than those of **TPR** dyes containing rhodanine-3-acetic acid units. Therefore, it seems that the rhodanine-3-acetic acid unit is not a suitable constructional moiety, although it increases the light-harvesting capability. The results therefore show that the **TPC** dyes with cyanoacrylic acid units give faster and more effective electron injection from their LUMOs to the CB of the TiO_2 than the **TPC** dyes with rhodanine-3-acetic acid units. Moreover, measurements by valence level spectroscopy, X-ray absorption spectroscopy and resonant photoemission spectroscopy for dye **D5** adsorbed on a TiO_2 surface reveal a dominating molecular surface configuration in which the dye molecules are bonded to the surface with the cyano moiety close to the TiO_2 substrate and the triphenylamino moiety pointing out from the surface. These results imply that the performances of DSSCs based on these dyes should, in addition to the energetics, also depend on the orientations, binding and sizes of the dyes on the TiO_2 surface. The IPCEs of these sensitizers are above 80%, and **TPC**-sensitized solar cells yield J_{sc} values of 13.90 ± 0.2 mA cm^{-2}, V_{oc} values of 740 ± 10 mV, and *ff* values of 0.70 ± 0.02, corresponding to η values of 7.20% under standard AM 1.5 sunlight. The photovoltaic performances of DSSCs based on the polyene dye classes **D**, **TPC** and **TPR** are summarized in Table 2.

Table 2. Absorption peaks of a series of **D**, **TPC** and **TPR** polyene dyes in THF and the photovoltaic performances of DSSCs based on them.

Dye	λ_{max}^{abs} [nm]	J_{sc} [mA cm^{-2}]	V_{oc} [V]	*ff*	η (%)
TPC1	438[a]	9.7	0.76	0.72	5.3
TPC2	441[a]	9.4	0.67	0.69	4.4
TPC3	444[a]	8.1	0.70	0.68	3.9
TPC4	425[a]	8.1	0.63	0.68	3.5
TPC5	500[a]	1.3	0.48	0.70	0.4
TPR1	468[a]	7.8	0.59	0.71	3.3
TPR2	478[a]	3.0	0.53	0.73	1.1
TPR3	480[a]	3.4	0.53	0.72	1.3
TPR4	464[a]	3.1	0.52	0.73	1.2
D5	441[b]	12.0	0.69	0.72	5.9
D7	441[b]	11.0	0.70	0.71	5.4
D9	462[b]	14.0	0.69	0.71	6.9
D11	458[b]	13.5	0.74	0.70	7.0

[a] In CH_2Cl_2. [b] In ethanol.

On the other hand, Ko and co-workers have reported new polyene dye sensitizers (**JK-57**, **JK-58** and **JK-59**, Figure 9) containing bis-dimethylfluorenyl amino groups as electron donors and cyanoacrylic acid units as electron acceptors bridged by phenylenevinylene units.[27] The absorp-

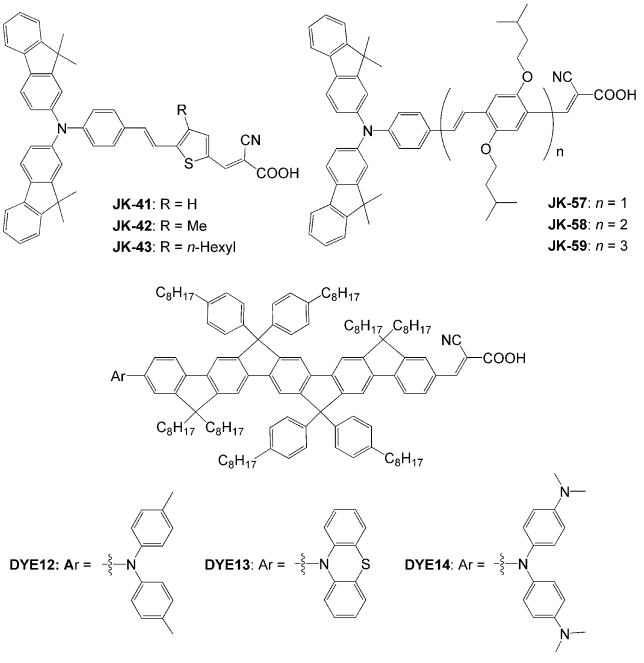

Figure 9. Molecular structures of polyene dye sensitizers **JK** and **DYE12**–**14**.

tion maxima shows red shifts in the order **JK-59** (λ_{max}^{abs} = 375 nm) > **JK-58** (λ_{max}^{abs} = 373 nm) > **JK-57** (λ_{max}^{abs} = 369 nm) due to the enlargement of the π conjugation systems by the phenylenevinylene components. The power conversion efficiency was quite sensitive to the conjugation lengths of the bridged phenylenevinylene groups. Under AM 1.5 solar conditions, the **JK-57**-sensitized cell gave a J_{sc} value of 10.50 mA cm^{-2}, a V_{oc} of 690 mV, and a *ff* of 0.73, corresponding to an η value of 5.34%. On the other hand, η values of 6.89% were obtained for **JK-58**-sensitized cells and 7.02% for **JK-59**-sensitized cells (for **JK-58**: J_{sc} = 13.26 mA cm^{-2}, V_{oc} = 700 mV, *ff* = 0.71; for **JK-59**: J_{sc} = 14.26 mA cm^{-2}, V_{oc} = 700 mV, *ff* = 0.70). The J_{sc} enhancement of **JK-58** and **JK-59** relative to **JK-57** can be related to the expansion of the π-conjugated system of the dyes. Moreover, Ko et al. reported that the polyene dyes **JK-41**

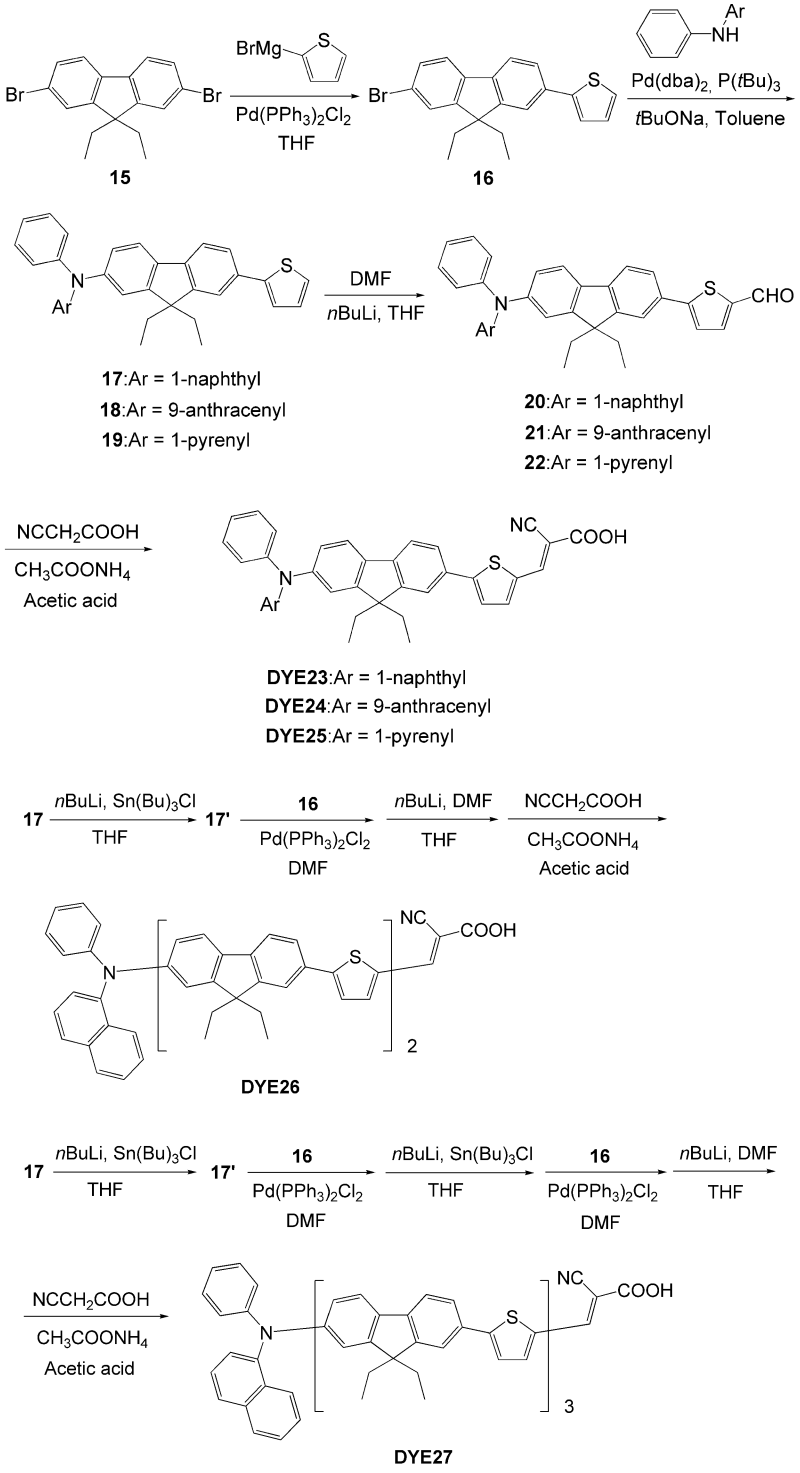

Scheme 3. Synthesis of polyene dye sensitizers **DYE23**–**27**.

(η = 7.69%), **JK-42** (η = 6.23%) and **JK-43** (η = 5.42%), containing thiophene rings, are also efficient sensitizers for DSSCs.[28]

Other new polyene-type dyes – fluorene-conjugated dye sensitizers **DYE23**–**27** (Scheme 3) containing conjugation bridges composed of alternating thiophene and fluorene units, diphenylamine as donor and cyanoacrylic acid as acceptor – were reported by Ho and Lin.[29] The dyes were constructed by the stepwise synthetic route illustrated in Scheme 3. From the compound **16**, the diarylamine-substituted fluorenylthiophene derivatives **17**–**19** were obtained by C–N coupling reactions involving Hartwig's catalyst[110] and the corresponding diarylamines. Thiophenaldehydes **20**–**22** were obtained by formylation of their corresponding thiophene derivatives **17**–**19**. The aldehydes **20**–**22** were then converted into **DYE23**–**27** by treatment with cyanoacetic acid in acetic acid in the presence of ammonium acetate. For the synthesis of **DYE26** and **DYE27**, the stannylene precursor **17′**, prepared by treatment of the lithium derivative of **17** with tributyltin chloride in THF, was used in a Stille coupling[111] with **16** to produce the bis(thienylfluorene)-conjugated analogue of **17**. This was then converted into the aldehyde, which on treatment with cyanoacetic acid produced **DYE26**. One more similar stepwise sequence starting with the bis(thienylfluorene)-conjugated analogue of **17** was executed to obtain the third-generation **DYE27**. A DSSC based on **DYE23** shows an η value of 5.23% with J_{sc} of 12.9 mA cm^{-2}, V_{oc} of 710 mV and *ff* of 0.74. The η values for **DYE24**–**27** are 2.86, 3.35, 3.89 and 3.80%, respectively. Recently, a series of ladder-type pentaphenylene-based dye sensitizers **DYE12**–**14** (η = 2.3, 1.8, and 1.1%, respectively) with long spacer bridged donor and acceptors and bulky alkylphenyl groups have also been reported by Müllen (Figure 9).[30]

3.1.3. Hemicyanine Dyes

Efficient hemicyanine dye sensitizers for DSSCs reported so far are D-π-A-type cationic dyes with *p*-dialkylaminophenyl groups as donor components, cationic moieties such as benzo- and naphthothiazolium, pyridinium, and indolium salts as strong acceptor parts, and methine (–CH=CH–) units as π conjugation bridges between the donor and acceptor parts (Figure 10).[33–37]

In 2000, Huang and co-workers reported the pyridinium hemicyanine dye sensitizers **QS** and **LQS**, containing sulfonate (-SO_3^-) anchoring groups. The overall yields were approximately doubled when the long alkyl chain was replaced by the methyl group. DSSCs with **LQS** displayed a broad feature with 33.8% of maximum IPCE and gave η values of about 2%.[33] In addition, Huang and co-workers designed and synthesized a series of new benzothiazolium hamicyanine dye sensitizers (**HC1**–**HC5**) containing sulfonate (-SO_3^-), carboxy (-COOH) or hydroxy groups as anchoring components and a naphthothiazolium hemicyanine (**HC6**) with both sulfonate and hydroxy groups.[34] These dyes exhibit absorption maxima at around 550 nm in solution. It was found that the IPCE spectra and the η values for DSSCs based on these hemicyanine sensitizers depended

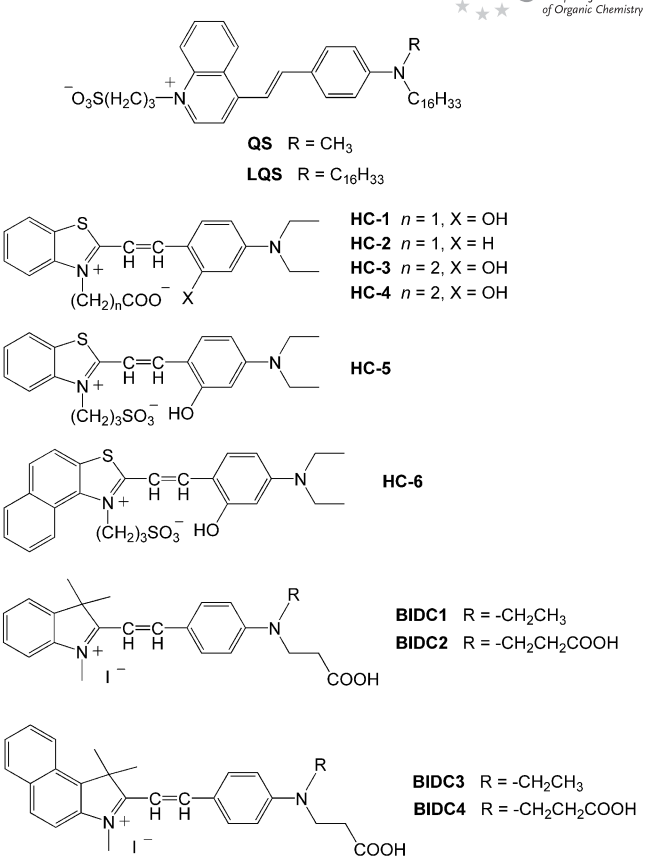

Figure 10. Molecular structures of hemicyanine dye sensitizers.

strongly on the type of anchoring group and decrease in the order: carboxy and hydroxy > carboxy > sulfonate and hydroxy, indicating the importance of anchoring groups for the photovoltaic performances of DSSCs. The highest conversion efficiency of 5.2% and IPCE of 74% were obtained for DSSCs based on **HC-1** under AM 1.5 solar conditions. The η values of **HC2**–**HC5** are 3.5, 4.4, 3.1, 2.0 and 2.6%, respectively. On the other hand, four indolium hemicyanine dyes (**BIDC1**–**4**) containing carboxy groups were synthesized. Interestingly, **BIDC2** (or **BIDC4**), bearing two carboxy groups, shows about two (or three) times more adsorption and a broader absorption spectrum on TiO_2 film than **BIDC1** (or **BIDC3**).[35] Consequently, of the four hemicyanine dyes, **BIDC4** generated the highest η value of 4.9%. The η values of **BIDC1**–**3** are 4.0, 4.6 and 4.4%, respectively.

3.1.4. Thiophene-Based Dyes

Thiophene- or oligothiophene-based dyes are also promising candidates as dye sensitizers in DSSCs because of their high chemical and environmental stabilities, as well as their strong photoabsorption properties and electronic tunability.[38–47] DSSCs based on some oligothiophene-based dye sensitizers (Figure 11) have been reported by Otsubo and Harima's group (**4T**-, **8T**-, and **12T-COOH**) and by Zhai and co-workers (**PTDA**).[38,39] The DSSCs based on **8T-COOH** and **PTDA** gave the η values of 1.3 and 3.3%, respectively. However, these oligothiophenes are liable to

experience dye aggregation through strong intermolecular π–π interactions, which is disadvantageous to photocurrent generation.

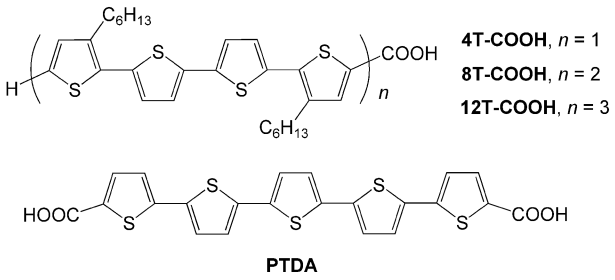

Figure 11. Molecular structures of oligothiophene-based dye sensitizers.

On the other hand, Koumura and Hara have recently designed and synthesized the new oligothiophene-based dyes **MK-1** and **MK-2** (Scheme 4), with carbazole moieties as donors, alkyl-functionalized oligothiophenes as π conjugation linkages and cyanoacrylic acid units as both acceptor and anchoring groups, based on the concept of the interface engineering of a dye-adsorbed TiO_2 surface, which can be controlled by the structural modification of the dye molecule to diminish charge recombination between the injected electrons and the dye cation and I_3^- ions and the aggregation of dye molecules. The synthetic routes to **MK-1** and **MK-2** are shown in Scheme 4.[40] The noteworthy feature of the dye structure is the presence of *n*-hexyl substituents on the oligothiophene linkages, preventing the approach of acceptors (i.e., dye cations and I_3^- ions) to the TiO_2 surface and also suppressing the aggregation of dye molecules through steric hindrance. High performances of DSSCs with **MK-1** and **MK-2** were thus achieved. A DSSC based on **MK-2** shows an η value of 7.7% with J_{sc} of 14.0 mA cm^{-2}, V_{oc} of 740 mV, and *ff* of 0.74. The IPCE is close in the visible region to 80%.

On the other hand, Ko and co-workers designed and synthesized the novel thiophene-based sensitizers **JK-45** and **JK-46** (Figure 12), consisting of: 1) a dimethylfluorenylamino moiety that not only acts as electron donor but also ensures greater resistance to degradation when exposed to light and/or high temperatures, 2) conducting thiophene units with aliphatic chains that enhance the interface and the water-tolerance in the electrolytes (I_3^-/I^-), and 3) a cyanoacrylic acid moiety, which acts as acceptor and anchoring group.[41] The visible absorption spectra of **JK-45** and **JK-46** each exhibit two maxima, at around 430 nm (ε = 34800 and 29200 dm^3 mol^{-1} cm^{-1} for **JK-45** and **JK-46**, respectively) and 370 nm (ε = 60200 and 35000 dm^3 mol^{-1} cm^{-1} for **JK-45** and **JK-46**, respectively), which are attributed to the π–π* transitions in the conjugated molecules. The LUMOs of **JK-45** and **JK-46** are much more negative than the CB of the TiO_2 (–0.5 V vs. NHE), thus providing a thermodynamic driving force for efficient electron injection. Molecular orbital (MO) calculations reveal that the HOMO of **JK-46** is localized over the fluorenylamino unit through benzo[*b*]thiophene and that the LUMO is localized over the cyanoacrylic unit through thiophene. This result indicates that HOMO to LUMO excitation moves the electron distribution from the bis(9.9-dimethylfluoren-2-yl)amino unit to the cyanoacrylic acid moiety, thus allowing efficient photoinduced electron transfer from the excited dye to the TiO_2 electrode. Moreover, **JK-70** and **JK-71**, with long alkyl chains on their dimethylfluorenylamino moieties, exhibited not only high photoconversion efficiency but also excellent stability under light soaking at 60 °C.[42] These results suggested that successful molecular design for DSSCs is achieved through the incorporation of long alkyl units into the dye skeleton, not only increasing the photoconversion efficiency but also exhibiting excellent stability under long-term light soaking. The photovoltaic performances of the DSSCs based on a series of **JK** dyes are summarized in Table 3.[43] As other thiophene-based dye sensitizers, **LJ1**, with triphenylamine and cyanoacrylic acid components bridged by 3,4-ethylenedioxythiophene (EDOT), and the oligothiophene-based dye **T1**, with diarylamine components at its 2- and 3-sites and a cyanoacrylic acid unit, exhibit high conversion efficiencies (η = 7.3 and 6.0% for **LJ1** and **T1**, respectively).[44,45]

On the other hand, with the goal of eliminating the dye desorption from the TiO_2 surface during long-term operation, Gratzel and co-workers designed and synthesized the novel organic sensitizer **C203** containing a fused dithienothiophene unit and possessing a high molar extinction coefficient ($\varepsilon = 44.8 \times 10^3$ dm^3 mol^{-1} cm^{-1}) at 525 nm.[46] This sensitizer was synthesized in three steps as depicted in Scheme 5. Suzuki coupling between **37** and (dithieno[3,2-*b*;2′,3′-*d*]thiophen-2-yl)boronic acid produced **38**, which was converted into its corresponding carbaldehyde **39** through a Vilsmeier–Haack reaction. The aldehyde **39** was condensed with cyanoacetic acid in a Knoevenagel condensation in the presence of piperidine to afford the target compound **C203**. The J_{sc}, V_{oc} and *ff* values under an irradiance of AM 1.5G full sunlight are 14.33 mA cm^{-2}, 734 mV and 0.76, respectively, yielding an η value of 8.0%.

3.1.5. Indoline Dyes

Indoline dye sensitizers, first reported in 2003 by Horiuchi and Uchida, are at present the most efficient organic sensitizers.[48] The designed novel indoline dye sensitizers **DYE40–45** (Figure 13) each consist of three important parts: 1) introduction of the rhodanine ring as the electron acceptor at the end of the dye structure contributed to the red shift in the absorption spectrum, the absorption maximum gradually being red-shifted with increasing numbers of rodanine rings from one to three, 2) the indoline moiety is a moderate electron donor, which is compatible with the rhodanine ring, and 3) the introduction of aromatic units on the indoline skeleton expanded the π conjugation in the dye and thus resulted in red-shifting of the absorption maximum and enhancement of the molar absorption coefficients. In fact, **DYE41**, with a 4-(2,2-diphenylvinyl)phenyl group, has a red-shifted absorption peak relative to **DYE40**,

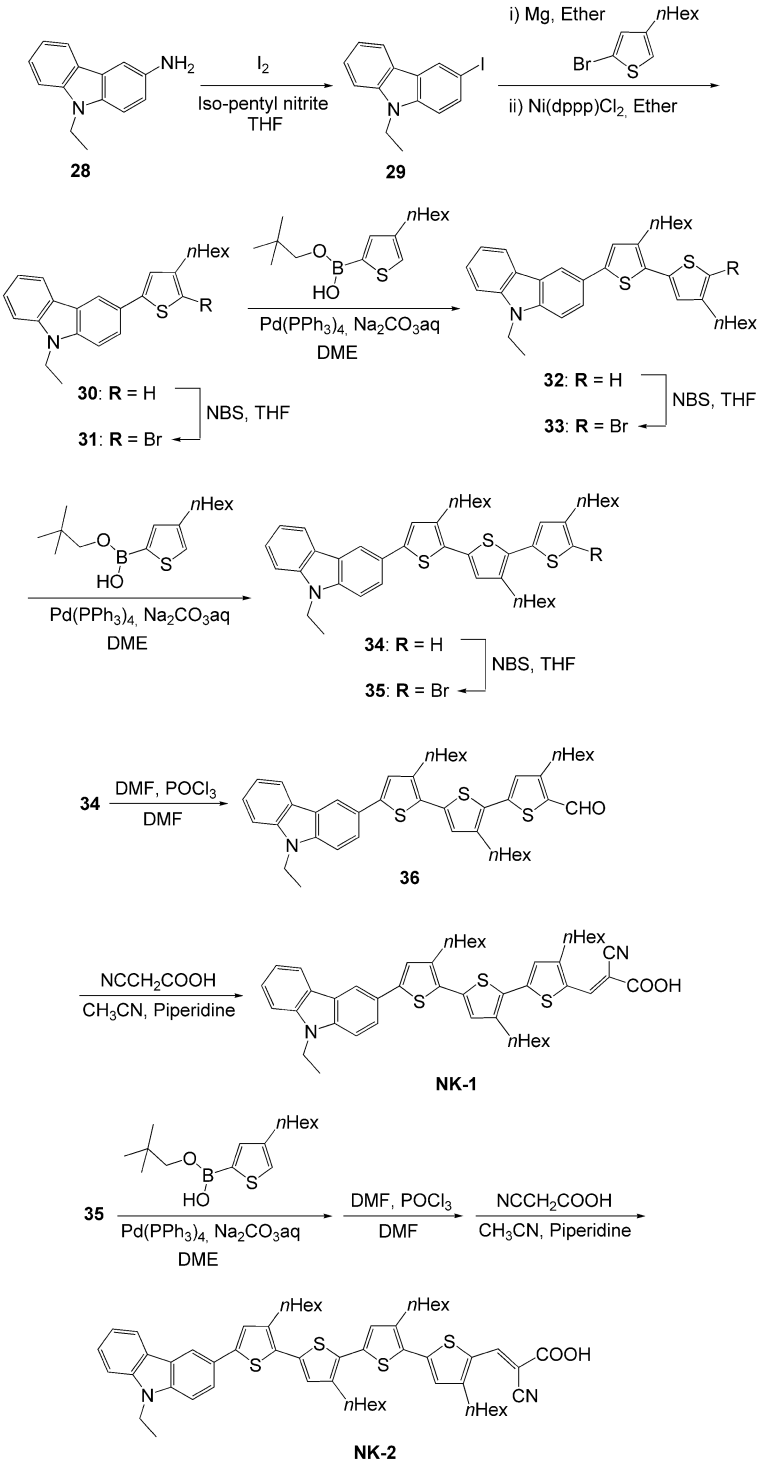

Scheme 4. Synthesis of thiophene-based dye sensitizers **MK-1** and **MK-2**.

with a 4-methoxyphenyl group, because **DYE41** has a more expanded π conjugation system (**DYE40**: λ_{max}^{abs} = 483 nm, ε = 43300 $dm^3 mol^{-1} cm^{-1}$, **DYE41**: λ_{max}^{abs} = 491 nm, ε = 55800 $dm^3 mol^{-1} cm^{-1}$). On the other hand, **DYE45** has a slightly red-shifted absorption spectra peak relative to **DYE42**–**44** (λ_{max}^{abs} = 526–532 nm), because **DYE45** has three rhodanine rings.

Furthermore, Grätzel and co-workers reported that the introduction of sterically hindered substituents such as *n*-octyl groups onto the rhodanine ring and the 4-(2,2-diphenylvinyl)phenyl group was effective in preventing dye aggregation and charge recombination (dark current) between I_3^- and injected electrons in the TiO_2 electrodes: the photovoltaic performance of the **D205** dye, containing an

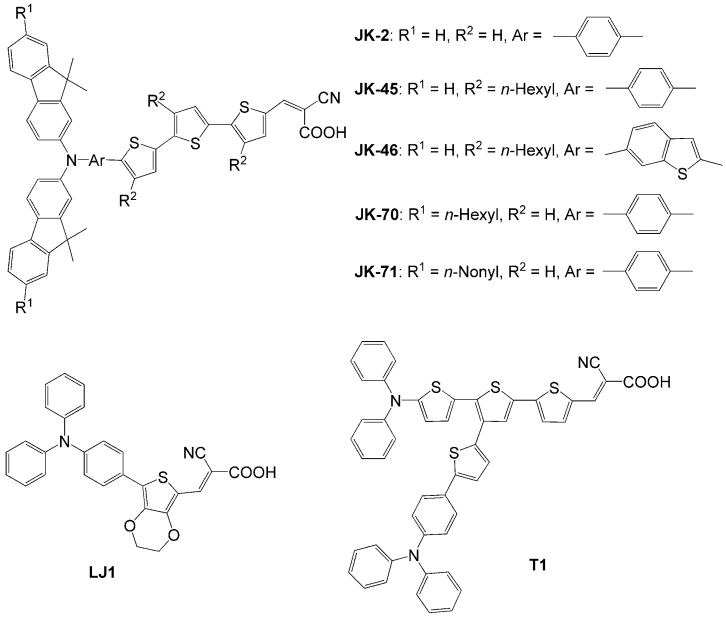

Figure 12. Molecular structures of thiophene-based dye sensitizers **JK-2**, **JK-45**, **46**, **70**, and **71** and of **LJ1** and **T1**.

Table 3. Absorption peaks of a series of thiophene-based **JK** dyes in THF and the photovoltaic performances of DSSCs based on them.

Dye	λ_{max}^{abs} [nm]	J_{sc} [mA cm^{-2}]	V_{oc} [V]	*ff*	η (%)
JK-2	364, 452	14.5	0.70	0.74	7.6
JK-45	369, 430	16.1	0.64	0.72	7.4
JK-46	372, 430	17.5	0.66	0.74	8.6
JK-70	367, 448	15.3	0.73	0.74	8.3
JK-71	368, 447	15.4	0.74	0.74	8.4

n-octyl group, is higher than that of **DYE42**, containing an ethyl group, so the improved values of V_{oc} and J_{sc} for **D205** can be attributed to the extension of the alkyl chain on the terminal rhodanine moiety from ethyl to octyl.[49] The synthetic route to **D205** is shown in Scheme 6. The photovoltaic performances of the DSSCs based on these indoline dyes are summarized in Table 4. A DSSC based on **D205** shows an η value of 9.5% with J_{sc} of 18.6 mA cm^{-2}, V_{oc} of 720 mV and *ff* of 0.72. The IPCE in the visible region is close to 80%. In addition to high efficiencies of DSSCs, indoline dyes have been shown by the reversible redox peaks in their cyclic voltammograms (CVs) to be highly stable to photoredox processes. Stability of the redox characteristics of a dye sensitizer is very important because one of the reasons for degradation of the performance is destruction of the dye through the formation of unstable radicals on light irradiation.

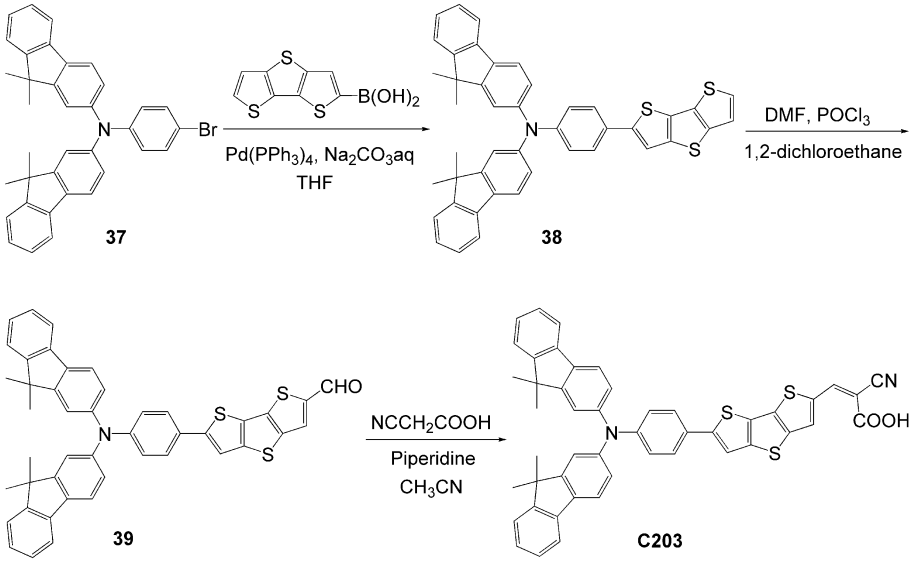

Scheme 5. Synthesis of thiophene-based dye sensitizer **C203**.

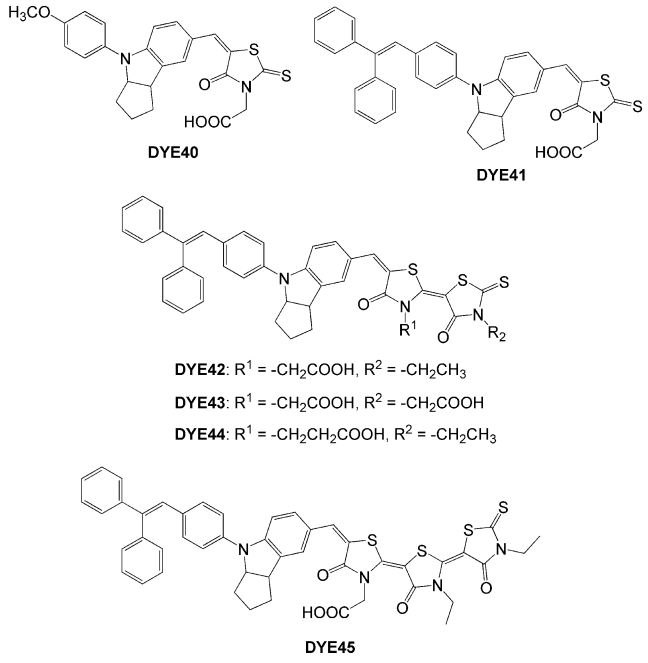

Figure 13. Molecular structures of indoline dye sensitizers **DYE40**–**45**.

as the electron acceptor. A number of researches have suggested that a carboxy group can form an ester linkage with a TiO_2 surface to provide a strongly bound dye and good electron communication between them. However, development of new donor–acceptor π-conjugated dyes for DSSCs is limited because for these reasons a carboxy group is required to combine with the π conjugation system or electron-accepting moiety of a dye. To obtain new and efficient D-π-A dyes for DSSCs, a novel molecular design principle, such as the establishment of a strong interaction between the electron-accepting moiety of the sensitizer and the TiO_2 surface is necessary. A series of novel donor–acceptor π-conjugated benzofuro[2,3-*c*]oxazolo[4,5-*a*]carbazole-type fluorescent dyes **OH1**–**4** (Figure 14) with carboxy groups at different positions on a chromophore skeleton have recently been designed as D-π-A dye sensitizers to meet the above requirements and have been synthesized by Ooyama and Harima.[50]

In dye **OH1**, a carboxy group acts not only as the anchoring group for attachment on the TiO_2 surface but also as the electron acceptor. For **OH2**, **OH3** and **OH4**, on the other hand, a carboxy group acts as an anchoring group, but the electron acceptor is not a carboxy group but a cyano group. The absorption (λ_{max}^{abs} = 415–430 nm, ε = 21500–26000 $dm^3 mol^{-1} cm^{-1}$) and fluorescence spectra (λ_{max}^{fl} = 525–540 nm, Φ = 0.97–0.99) and the cyclic voltammograms of the fluorescent dyes resemble one another very closely, showing that the position of the carboxy group has a negligible influence on the photophysical and electrochemical properties of these dyes. MO calculations showed that the absorption bands of the dyes were mainly attributable to the transitions from HOMO to LUMO, with the HOMOs mostly being localized on the 3-dibutylamino-benzofuro[2,3-*c*]oxazolo[4,5-*a*]carbazole components for all dyes, and LUMOs mostly being localized on the carboxyphenyl moiety for **OH1** and the cyanophenyl moieties for **OH2**, **OH3** and **OH4**, revealing strong intramolecular charge transfer from the 3-(dialkylamino)benzofuro[2,3-*c*]oxazolo[4,5-*a*]carbazole moieties to the carboxylphenyl or cy-

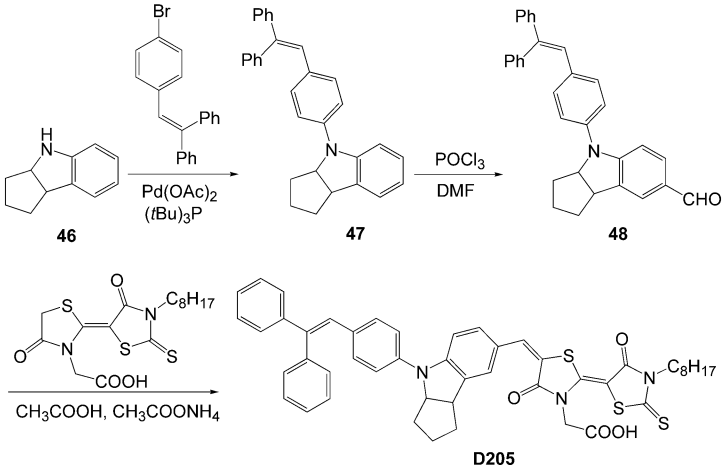

Scheme 6. Synthesis of indoline dye sensitizer **D205**.

Table 4. Photovoltaic performances of DSSCs based on indoline dyes.

Dye	J_{sc} [mA cm^{-2}]	V_{oc} [V]	*ff*	η (%)
DYE40	14.8	0.59	0.59	5.1
DYE41	17.8	0.60	0.57	6.1
DYE42	18.8	0.65	0.54	6.5
DYE43	17.5	0.58	0.54	5.5
DYE44	17.4	0.63	0.51	5.6
DYE45	19.6	0.57	0.53	5.9
D205	18.6	0.72	0.72	9.5

3.1.6. Heteropolycyclic Dyes

As mentioned above, many donor–acceptor π-conjugated (D-π-A) dyes have a carboxy group acting not only as anchoring group for attachment on the TiO_2 surface but also

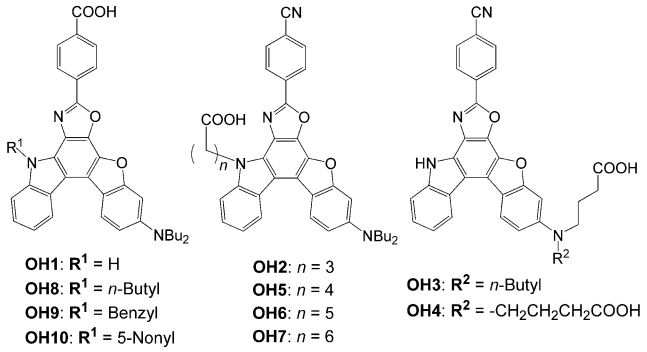

Figure 14. Molecular structures of heteropolycyclic fluorescent dye sensitizers **OH1**–**10**.

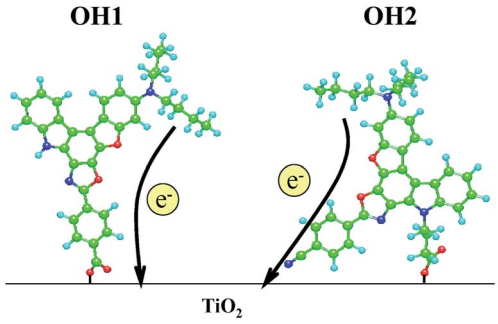

Figure 15. Plausible configurations of **OH1** and **OH2** on TiO_2 surface. Light blue, green, blue, and red balls correspond to hydrogen, carbon, nitrogen and oxygen atoms, respectively.

anophenyl moieties on photoexcitation for all dyes. When these dyes are used in dye-sensitized solar cells, however, their photovoltaic performances are very different. The photovoltaic performance of **OH2**, with a non-conjugated linkage between carboxy group and chromophore, is similar to that of **OH1** and better than those of **OH3** and **OH4**. From the results of the MO calculations and the photovoltaic performances, for **OH1** electrons will be injected from dye to TiO_2 through the carboxy group. On the other hand, from the molecular structure of **OH2** it was suggested that the phenylcyano group, acting as an electron acceptor, is located in close proximity to the TiO_2 surface through interactions such as intermolecular hydrogen bonding between the cyano nitrogen of the dye and the hydroxy proton of the TiO_2 surface. Consequently, dye **OH2** can efficiently inject electrons from the phenylcyano group to the conduction band of the TiO_2 electrode through the intermolecular hydrogen bonding (Figure 15). On the other hand, they presume that free rotation of the butyl group in **OH3** and rigid linkages with the TiO_2 surface in **OH4** prevent the phenylcyano moiety of the dye from being in close proximity to the TiO_2 surface. In order to provide further confirmation for this view, the dyes **OH5**–**7** (Figure 14) with different lengths of nonconjugated alkyl chains containing carboxy groups at their end positions were designed and synthesized.[51] It was found that in spite of the lengths of the alkyl chains, because of their flexibilities the cyano groups on the dyes were located in close proximity to the TiO_2 surface, so good electron communication between the dyes and the TiO_2 surface was established. It was concluded that a carboxy group in a donor–acceptor π-conjugated sensitizer is necessary not as the electron-acceptor, but only as an anchoring group for attachment on the TiO_2 surface. Therefore, it was suggested that the most important element for the development of new and efficient donor–acceptor π-conjugated sensitizers for DSSCs is to design dye molecules capable of strong interaction between the electron-acceptor moiety of the sensitizer and the TiO_2 surface.

Furthermore, it has been demonstrated that donor–acceptor π-conjugated fluorescent dyes exhibiting solid-state fluorescence can be a class of potential sensitizers for DSSCs. In general, D-π-A fluorescent dyes in the solid state undergo fluorescence quenching through molecular aggregation. The introduction of bulky substituents on the fluorophore skeleton and the construction of nonplanar structures with sterically hindered substituents are known to be very useful methods for solving the problem of fluorescence quenching by aggregation. Donor–acceptor π-conjugated benzofuro[2,3-*c*]oxazolo[4,5-*a*]carbazole-type fluorescent dyes (**OH1**, **OH8**–**10**, Figure 14) designed around this concept, with substituents (R = H, butyl, benzyl, and 5-nonyl) on the carbazole ring nitrogen, were synthesized as sensitizers in DSSCs.[52] The solid-state fluorescence properties of these dyes were changed through the introduction of bulky substituents in the dye skeletons. The fluorescent dyes **OH9** (R = benzyl) and **OH10** (R = 5-nonyl) with bulky substituents exhibited strong solid-state fluorescence properties. This result showed that the bulky groups reduced the π–π interaction between the dyes and prevented the fluorescence quenching in the molecular aggregation state. The photovoltaic parameters of DSSCs based on these dyes were measured, and it was found that the **OH10** exhibited 100% efficiency for absorbed photon-to-current conversion, demonstrating that the bulky 5-nonyl group in **OH10** can efficiently prevent intermolecular energy transfer between the dyes in molecular aggregation states. DSSCs based on the benzofuro[2,3-*c*]oxazolo[4,5-*a*]carbazole-type fluorescent dyes **OH1**–**10** showed η values of 1.0–1.5%.

3.2. Xanthene Dyes

Xanthene dyes such as mercurochrome, eosin Y, fluorescein, Rose Bengal and rhodamine 6G are commercially available at low cost and were employed as sensitizers in early DSSCs.[53–56] However, the photovoltaic performances of DSSCs based on the xanthene dyes are low because of their narrow absorption bands and instabilities. The η values of DSSCs based on eosin Y and mercurochrome (Figure 16) are 1.3% and 1.4%, respectively.[53,54] Yanagida and Fukuzumi reported that a DSSC based on the fluorescein derivative **DPAX**, made up of an electron donor (diphenylanthracene) unit and an acceptor unit (difluoroxanthene), had an η value of 0.85%.[55] Recently, a new class of chalcogenoxanthylium dyes (**1-E**, **2-E**, **4-Se**) for applications in DSSCs has been reported by Detty and Watson. The H-

Aaggregated dyes on TiO_2 surfaces exhibited increased light-harvesting efficiencies and IPCE values. The IPCEs of the dyes **1-E** ranged from 70% to 84%.[56]

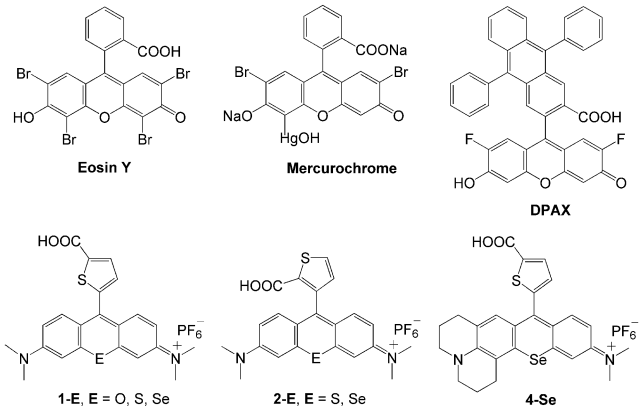

Figure 16. Molecular structures of xanthene dye sensitizers.

3.3. Perylene Dyes

Perylene dyes (Figure 17) have received much attention as interesting sensitizers for DSSCs thanks to their outstanding chemical, thermal and photochemical stabilities and their high molar absorption coefficients in the long-wavelength region (at around 600 nm). In the early stages of DSSC work based on perylenedicarboxylic acid anhydride and its derivatives, Ferrere and Gregg obtained the following results:[58] 1) the introduction of amino group at the 9-position led to a red-shift of the absorption maxima and improvement in photoconversion efficiency, due to the electron-donating effect of amino substitution, and 2) perylene dicarboxylic acid anhydride shows a blue-shifted absorption when adsorbed onto TiO_2. This effect is attributed to the ring-opening of the anhydride group on the perylene to form two carboxylates, which provides strong chemical interactions with the TiO_2 surface and effective electronic coupling. The dicarboxylic acid anhydride moiety is thus the best anchoring group for this type of sensitizers. A DSSC based on **P2** showed an η value of 1.9%.

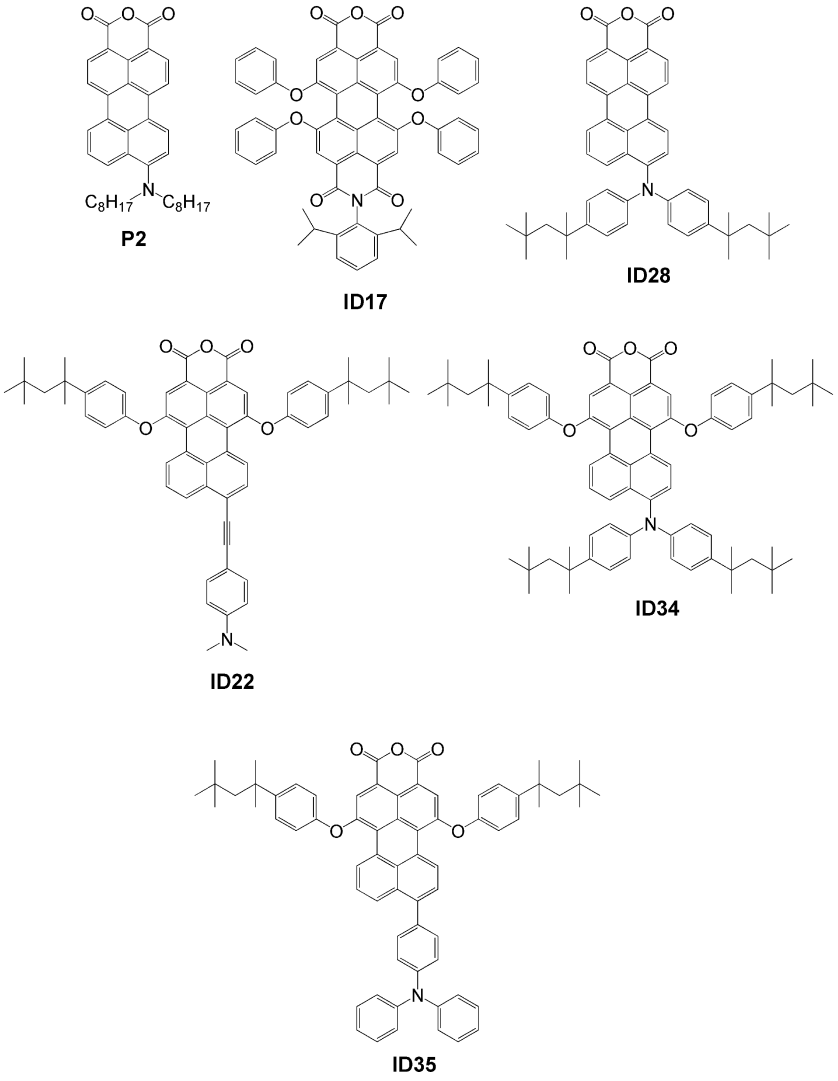

Figure 17. Molecular structures of perylene dye sensitizers.

Novel perylenedicarboxylic acid anhydrides (**ID17**, **ID22**, **ID28**, **ID34** and **ID35**, Figure 17) with ICT character due to substituents of different donor strengths (diphenylamino, *p*-diphenylaminophenyl and *p*-(dimethylamino)phenylethynyl) were synthesized by Edvinsson and co-workers.[59] For **ID22**, **ID28**, **ID34** and **ID35**, with the stronger donors relative to **ID17**, they obtained shifts of both the LUMOs and the HOMOs to more negative potentials, together with increases in the charge separations in the excited dyes. On going from **ID17** → **ID22** → **ID28**, a monotonic decrease in the absorption coefficients and a red-shift in the onsets of absorption were observed, because of increasing donor strength. By comparing **ID34** (λ_{max}^{abs} = 599 nm, ε = 32000 $dm^3 mol^{-1} cm^{-1}$) and **ID28** (λ_{max}^{abs} = 605 nm, ε = 21000 $dm^3 mol^{-1} cm^{-1}$) they showed that the introduction of phenoxy substituents in the bay position of the perylene core led to the improvement of the absorption coefficient. From the experimental studies and time-dependent density functional theory (TD-DFT) calculations they concluded that the ICT character increased in the order **ID34/ID28** > **ID22** > **ID35** > **ID17**. The η value increased in the order **ID34/ID28** (3.2%/3.9%) > **ID22** (2.4%) > **ID35** (2.0%) > **ID17** (1.4%), following the trend of the ICT values above. The same trend was also observed in the J_{sc} values (8.0 / 10.4, 7.5, 6.1 and 7.3 $mA cm^{-2}$ for **ID34/ID28**, **ID22**, **ID35** and **ID17**, respectively). The photocurrents were improved remarkably with increasing ICT character of the dyes. They inferred that these donors act in two ways: i) generally raising the LUMO energy levels, thus providing more efficient injection of electrons into the CB of the TiO_2, and ii) successively improving the intramolecular charge separation in the dye, promoting more effective electron injection into TiO_2 in competition with prevention of the undesired recombination of electrons from the TiO_2 with the oxidized dye.

More recently, Nazeeruddin and co-workers have reported the highly efficient novel perylene sensitizer **DYE53** (λ_{max}^{abs} = 506 nm when adsorbed on TiO_2, Scheme 7) with two thiophenol groups, which yields 87% IPCE and an η value of 6.8% with J_{sc} = 12.60 ± 0.20 $mA cm^{-2}$, V_{oc} = 728 ± 15 mV and *ff* = 0.74 ± 0.01 under standard AM 1.5 solar conditions.[60] As shown in Scheme 7, a high yield of **DYE53** is prepared in four steps.

On the other hand, several solar cells sensitized with perylene imides have been reported, but the η values remain low in comparison with those obtained with other organic dyes.[61] The origin of the low performance is not only the poor electron-donating abilities of the perylene dyes, which makes it difficult to inject electrons from the excited perylene dyes into the CB of the TiO_2 electrode efficiently, but also the aggregation of dyes on the TiO_2 surface. The novel perylene imide derivative ***i*Pr-PMI** (Figure 18), with a strongly electron-donating moiety, bulky substituents and an acid anhydride as a strong coupling group for dye-sensitized solar cells, has been designed and synthesized, and an η value of 2.6% was reported by Imahori and co-workers in 2007.[62] The following points were considered in the molecular design. 1) Multiple strongly electron-donating substituents (i.e., two pyrrolidines) at the perylene core considerably shift the first oxidation potential in the negative direction, so efficient electron injection from the excited singlet state into the CB of the TiO_2 electrode is to be expected, leading to high photocurrent generation; furthermore, such substitution should vary the light-harvesting capability in the red-to-NIR region). 2) The degree of dye aggregation on the TiO_2 electrode can be modulated by the substituents (i.e., 2,6-diisopropylphenyl and cyclohexyl groups) at one imide end. It should be noted that the electronic structures of the perylene π-systems are not affected by the substituents at the imide nitrogen because the frontier orbitals of these compounds have nodes at the imide nitrogen and the anhydride oxygen atoms. 3) The natures of the anchoring groups (i.e., acid anhydride and carboxylic acid) and the electronic coupling between the perylene core and the TiO_2 surface should greatly affect the cell performance.

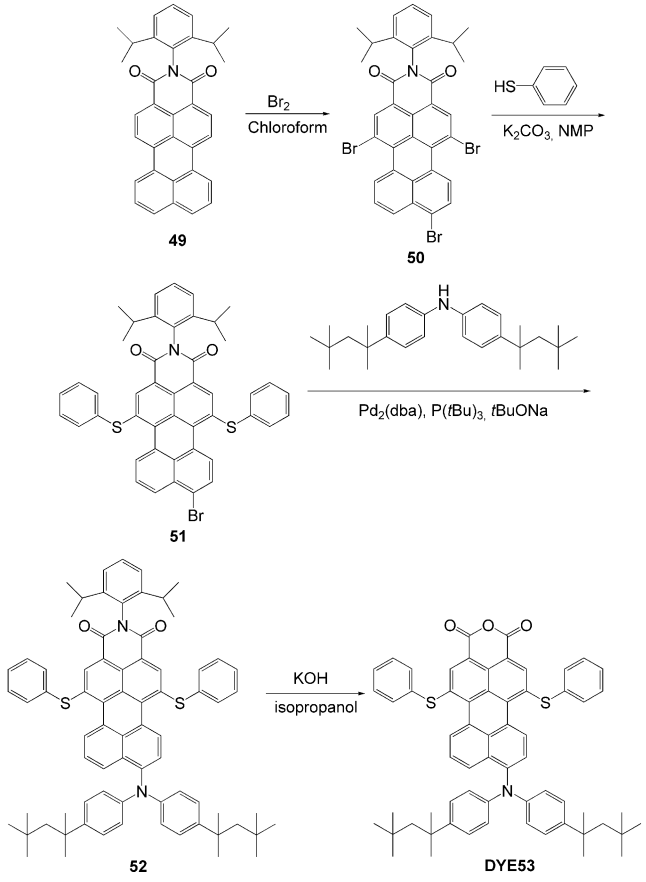

Scheme 7. Synthesis of perylene dye sensitizer **DYE53**.

The η value reported for the ***i*Pr-PMI** cell (2.6%) is ca. 70% greater than that for the **Cy-PMI** cell (1.5%), showing that the larger substituent at the imide nitrogen inhibits the dye aggregation on the surface of the TiO_2, leading to suppression of the unfavourable deactivation of the excited state of the dye. The η value for the ***i*Pr-PMI**-sensitized solar cell (2.6%) is remarkably high in comparison with that (<0.1%) for the TiO_2 cell with the similar **PMI** derivative

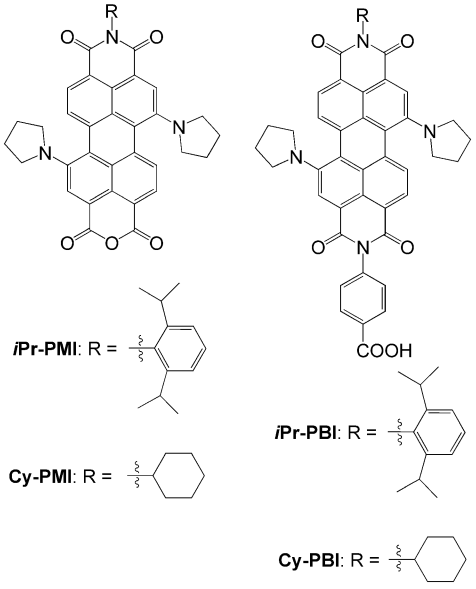

Figure 18. Molecular structures of perylene imide sensitizers ***i*Pr-PMI**, **Cy-PMI**, ***i*Pr-PBI** and **Cy-PBI**.

without an electron-donating substituent. It should be emphasized here that the η value for the ***i*Pr-PMI**-sensitized solar cells is the largest one out of the perylene imide-sensitized solar cells. The excited singlet state of the perylene imide dye with substituents that are both strongly electron-donating and bulky can thus inject electrons into the CB of the TiO_2 electrode, resulting in the efficient photocurrent generation. On the other hand, the η values for the ***i*Pr-PBI**- and **Cy-PBI**-sensitized solar cells (<0.02%) are smaller than those for the ***i*Pr-PMI**- and **Cy-PMI**-sensitized solar cells. More importantly, comparison of ***i*Pr-PMI** and ***i*Pr-PBI** shows that changing the coupling moiety to the TiO_2 electrode yields a remarkable difference in device performance, despite the fact that both electron-donating and sterically hindering groups are present in both molecules. Such a large difference may be explained by the difference in the electronic coupling between the dyes and TiO_2. The smaller electronic coupling between the perylene core and the TiO_2 surface through the carboxyphenyl group in the **PBI** would be responsible for the slow electron injection from the excited **PBI** to the CB of the TiO_2 electrode, leading to the extremely low η values. The coupling group between the perylene core and the TiO_2 electrode is thus of utmost importance in determining dye performance.

3.4. Porphyrin Dyes

Chlorophylls (**Chls**) and porphyrins have been regarded as promising candidates for photosensitizers for DSSC due to their strong Soret (400–450 nm) and moderate Q band (550–600 nm) absorption properties. As a pioneering work for DSSCs based on **Chl** derivatives and related porphyrins, Grätzel and Kay obtained IPCE values of over 80% and an η value of 2.6% for a TiO_2 electrode sensitized with copper mesoporphyrin **IX** (Figure 19).[63] Most recently, a DSSC fabricated by Wang and Koyama by use of **Chl c_2** exhibited J_{sc} = 13.7 mA cm^{-2}, V_{oc} = 570 mV and η = 4.6%.[64] On the other hand, for photovoltaic cells with **H_2TCPP**, Cherian and Wamser have reported IPCE values of 25–55% and η of 3%.[65]

However, the η values of porphyrin-sensitized solar cells are much smaller than those of other organic dye-sensitized solar cells. Recently, Durrant and co-workers compared the electron injection and charge recombination properties of **N3**, free-base **H_2TCPP** and **Zn-TCPP** on TiO_2.[66] They showed that these three dyes have almost indistinguishable electron injection and recombination kinetics, and revealed that the lower efficiency of porphyrin sensitizers is the result of the increased probability of exciton annihilation from close porphyrin proximity, because porphyrins have an inherent tendency to aggregate. On the other hand, some researchers assigned the poor performances of porphyrin-sensitized solar cells to their insufficient light-harvesting properties in the visible range (lack of any absorption band between 450 and 550 nm) and effects of electronic coupling between the porphyrin and the TiO_2 surface, as well as the formation of molecular aggregates.[67–69,73–76]

Palomares and co-workers have shown that the presence of *p*-hydrophobic alkyl substituents on *meso*-phenylporphyrins (see **FbP2** in Figure 19) not only inhibits the formation of molecular aggregates but also decreases recombination between the photo-injected electrons at the TiO_2 electrode and the electrolyte (I_3^-).[67] On the other hand, the coordination of metal ions in the porphyrin core can influence the electron transfer process between the chromophore and the CB of the TiO_2. In addition, the metallation affects the chemical and physical properties of porphyrins. The effects of the central metal in methylphenyl-carboxyphenylporphyrin (**P_M**) on photocurrent generation were examined by Otero and co-workers.[68] They showed that the photocurrent quantum yield – that is, the charge-injection yield (Φ_{inj}) multiplied by the charge-collection efficiency (η_c) – increased when the one electron-oxidation potential (E_{ox}) was increased (i.e., a negative shift in the HOMO), which was ascribed to the suppression of reverse electron transfer from TiO_2 to the metalloporphyrin sensitizer. In addition, it was shown by Nazeeruddin et al. that Zn porphyrins exhibit much better performance than Cu porphyrins. Out of the tetraphenylporphyrin-type compounds, tetraxylporphyrinato Zn^{II} ethenyl benzonic acid (**ZnTXPSCA**) showed the best performance: J_{sc} = 9.7 mA cm^{-2}, V_{oc} = 660 mV and η = 4.8%.[69]

The performances of a wide variety of porphyrins were compared for a review of porphyrin-sensitized solar cells, and their structural dependence was analyzed by Officer et al.[70] They showed that the β-pyrrolic-substituted **Zn**-porphyrin monoacids (see **BetaP** in Figure 20)[71] performed considerably better than all the *meso*-substituted porphyrin dyes (see **MesoP** in Figure 20).[72] The superior performance of **BetaP** suggests that the mode of binding is an important factor in determining the cell performance. They also evaluated the value of the conjugative linkage between the por-

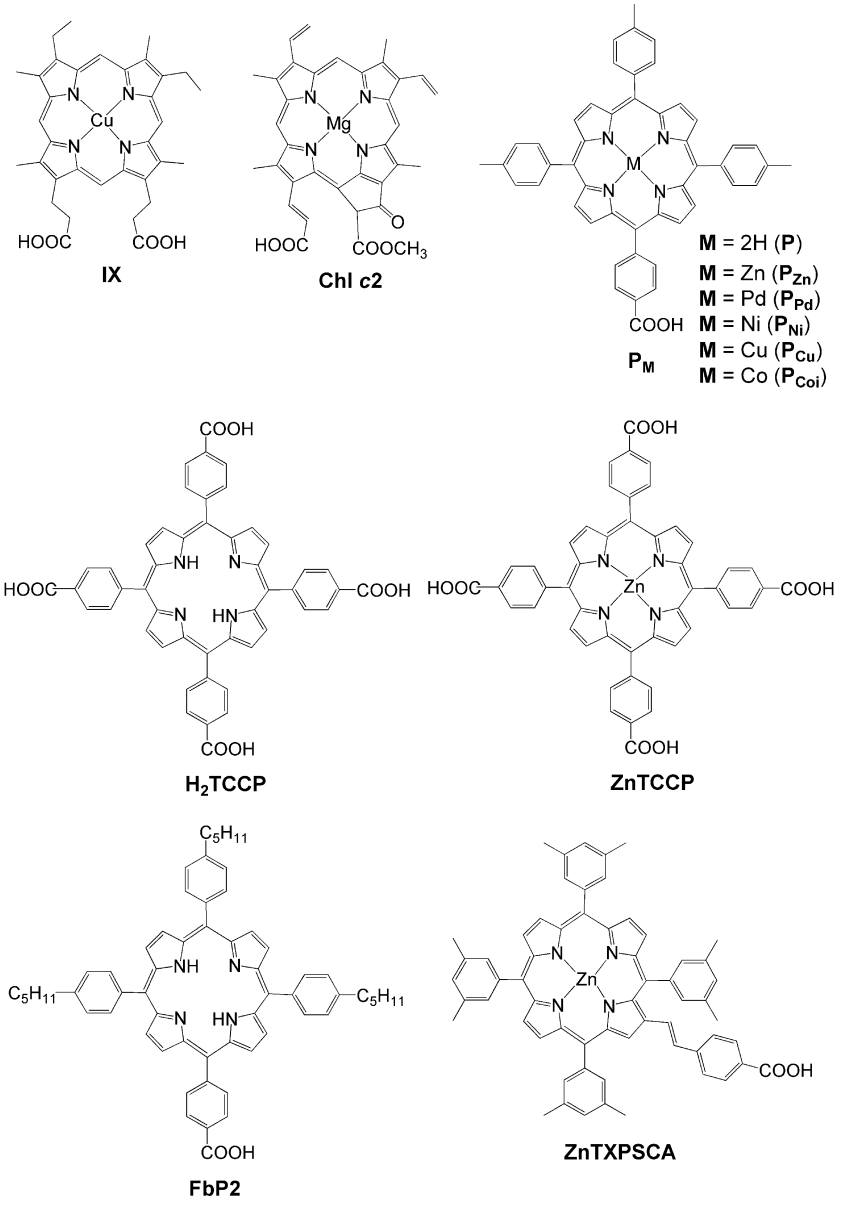

Figure 19. Molecular structures of porphyrin dye sensitizers.

phyrin and the binding group and demonstrated that the nature of the carboxylic acid linker to the porphyrin has a significant influence on the light-harvesting and photovoltaic properties. The conjugative linkage was responsible for the improved light-harvesting performance of these β-pyrrolic-substituted carboxy-functionalised porphyrins over the *meso*-arylcarboxy-functionalised porphyrins. In addition, it is well known that extension of the porphyrin π-system by modification of a β-pyrrolic position with an olefinic linkage is an effective method for broadening the absorption window (see R^2 of **BetaP** in Figure 20). Therefore, for the conjugated linkers at the β-pyrrolic position, the number of double bonds or the presence of the phenyl moiety caused enhancement and red shifts of the absorption bands, but made no significant difference in overall cell performance.

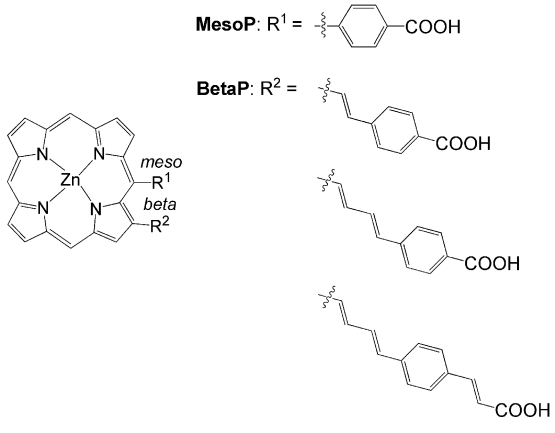

Figure 20. Molecular structures of β- and *meso*-substituted **Zn**-porphyrin sensitizers.

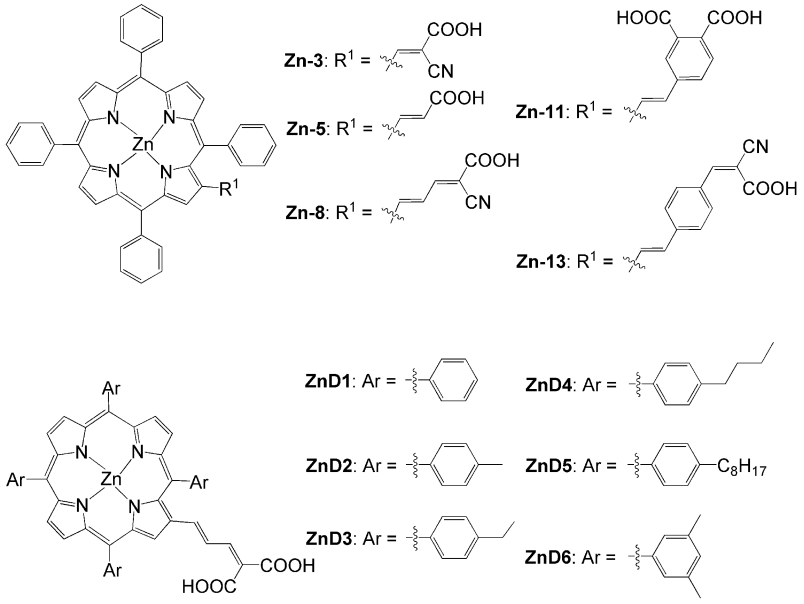

Figure 21. Molecular structures of porphyrin dye sensitizers **Zn-3**, **Zn-5**, **Zn-8**, **Zn-11**, **Zn-13** and **ZnD1**–**6**.

A series of Zn tetraphenylporphyrins (**Zn-3**, **Zn-5**, **Zn-8**, **Zn-11** and **Zn-13**) each containing a conjugated peripheral chain with a carboxy end were synthesized, their absorption and redox properties were determined, and their performances as dye sensitizers were examined by Grätzel and co-workers (Figure 21).[73] The solar cell sensitized with (tetraphenylporphyrinato)zinc-cyanoacrylic acid (**Zn3**) yielded the following remarkable performance: the maximum IPCE = 85%, J_{sc} = 13.5 mA cm^{-2}, V_{oc} = 560 mV, and η = 5.2%. The η values of **Zn5**, **Zn8**, **Zn11** and **Zn13** were 4.0, 4.0, 2.4 and 3.7%, respectively. More recently, in an attempt to improve the efficiencies of these dyes further, these workers designed and synthesized the novel porphyrin sensitizers **ZnD1**–**6**, in which the aryl groups act as electron donors and the malonic acid binding groups as acceptors.[74] The photovoltaic performances of the DSSCs based on these porphyrin sensitizers are summarized in Table 5. All six porphyrin dyes gave solar cell efficiencies of ≥5%, but the best performing dye **ZnD2** gave a J_{sc} of 14.0 ± 0.20 mA cm^{-2}, a V_{oc} of 680 ± 30 mV and an *ff* value of 0.74, corresponding to an η of 7.1%. The IPCE in the visible is over 80%; this is the most efficient porphyrin-sensitized solar cell reported to date. It has therefore been shown that there is a strong interaction between the porphyrin π-system and an olefin-linked electron acceptor substituted at the β-pyrrolic position of the porphyrin ring, and that the malonic acid group facilitates stronger binding to the TiO_2 surface with a consequent improvement in the electronic coupling of the dye.

Table 5. Photovoltaic performances of DSSCs based on porphyrin sensitizers **ZnD1**–**6**.

Dye	J_{sc} [mA cm^{-2}]	V_{oc} [V]	*ff*	η (%)
ZnD1	12.1	0.64	0.66	5.1
ZnD2	14.0	0.68	0.74	7.1
ZnD3	14.8	0.64	0.63	5.8
ZnD4	13.4	0.70	0.68	6.4
ZnD5	13.4	0.65	0.61	5.3
ZnD6	13.3	0.69	0.68	6.1

Recently, Imahori and co-workers reported that elongation of the π-system and lowering of the symmetry, as in the *meso*- and β-naphthalene-fused porphyrincarboxylic acid **fused-Zn-1** (Scheme 8), caused red-shifting of absorption bands (the Soret and Q bands) and gave an η value improved by 50% relative to the nonfused porphyrin **Zn-1**.[75] They designed the novel unsymmetrically π-elongated porphyrin **fused-Zn-1** on the basis of the following concepts: 1) the unsymmetrically π-elongated porphyrin would be expected to collect visible light efficiently, leading to improvement of the photovoltaic properties, and 2) in order to facilitate electron injection from the porphyrin excited singlet state to the CB of the TiO_2 electrode, a carboxy group is attached to the fused naphthyl moiety in the porphyrin ring. Bulky mesityl groups are also introduced at the three *meso* positions of the porphyrin ring to reduce the aggregation of the porphyrin molecules on the TiO_2 surface. The synthetic route to **fused-Zn-1** is shown in Scheme 8. Firstly, 5-[(4-methoxycarbonyl)naphth-1-yl]-10,15,20-tris-(2,4,6-trimethylphenyl)porphyrin (**H_2-1**) was synthesized by cross-condensation of mesityldipyrromethane with 4-(methoxycarbonyl)naphthylaldehyde and 2,4,6-trimethylbenzaldehyde. Ni^{II}-Metallation was carried out by treatment of **H_2-1** with $Ni(acac)_2$ to yield **Ni-1**. Ring-closure was achieved by treatment of **Ni-1** with $FeCl_3$. Subsequent demetallation, hydrolysis and Zn^{II}-metallation gave **fused-Zn-1**. The porphyrin reference **Zn-1** was also prepared from **H_2-1**. A **fused-Zn-1**-sensitized solar cell exhibited an η value of 4.1%, which was an improvement by 50% relative to

the unfused porphyrin **Zn-1**-sensitized solar cell (η = 2.8%). These results clearly show that the elongation of a porphyrin π system with low symmetry is a useful tactic for collecting solar light in the visible and NIR, leading to improved cell performance of porphyrin-sensitized solar cells.

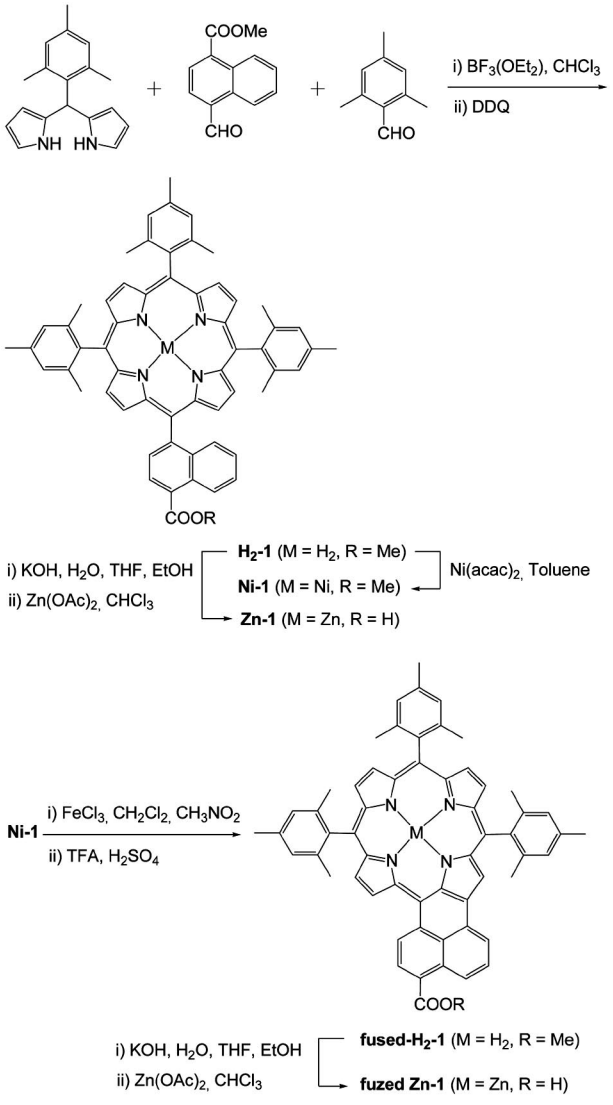

Scheme 8. Synthesis of porphyrin dye sensitizers **Zn-1** and **fused-Zn-1**.

Moreover, quinoxalino[2,3-β]porphyrinmono- and -dicarboxylic acids (**ZnQMA** and **ZnQDA**, Figure 22) have been synthesized to evaluate the effects of β,β′-carboxyquinoxalino moieties on the optical, electrochemical and photovoltaic properties of the porphyrins.[76] The **ZnQMA**-sensitized solar cell displays an η value of 5.2%, whereas the **ZnQDA**-sensitized solar cell shows an η value of 4.0%. The superior performance of the **ZnQMA**-sensitized solar cell over the **ZnQDA**-sensitized one originates both from the more favourable electron injection and from better charge collection efficiency.

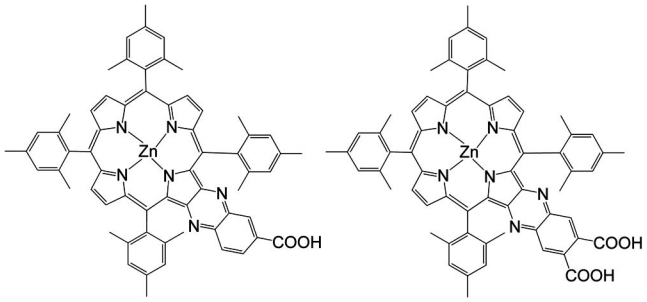

Figure 22. Molecular structures of porphyrin dye sensitizers **ZnQMA** and **ZnQDA**.

3.5. Merocyanine Dyes

Some merocyanine dyes form J- and H-aggregates on the surfaces of TiO_2 electrodes. The J-aggregates show absorption shifts to the longer-wavelength region and the H-aggregates show shifts to the shorter-wavelength region, in relation to the absorption of the monomeric forms.[112] The relationship between dye aggregation on the TiO_2 surface and the photoelectrochemical properties is very interesting. Kamat and co-workers reported the photophysical properties and photovoltaic performances of merocyanine 540 (**MC540**, Figure 23).[77] They demonstrated that the IPCE for the monomeric form (ca. 40%) is nearly five times greater than that for the H-aggregate form (ca. 8%), showing that H-aggregates of the merocyanine dye **MC540** are less efficient than its monomer counterpart in sensitizing TiO_2 nanoparticles. In contrast, Arakawa and co-workers reported on the photoelectrochemical properties of TiO_2 electrodes sensitized by a new series of benzothiazole merocyanine dyes (**Mc[*m*,*n*]**) possessing long, straight alkyl chains (carbon number: m = 2, 5, 10, 18 and 20) and different methylene chain lengths (carbon number: n = 1, 3 and 5) between the carboxy group and the dye chromophore (Figure 23).[78] In those reports, they found that the benzothiazole merocyanine dyes (**Mc[*m*,*n*]**) formed J-aggregates on TiO_2 surfaces and that the J-aggregates of merocyanine possessing long alkyl chains showed high photosensitization efficiency. It has been demonstrated that the formation of J-aggregates is more facile with increasing alkyl chain length. The J-aggregates of the dyes with long alkyl chains showed excellent capabilities for sensitization on TiO_2 electrodes. Consequently, the η and IPCE values increased with increasing length of alkyl chain (m) attached to the benzothiazole ring. In addition, the IPCEs decreased significantly with increasing methylene length (n) between the carboxy anchoring group and the dye chromophore. It was suggested that the photocurrent increased with decreasing distance between the dye chromophore and the TiO_2 surface because of efficient charge transfer through this short distance. Among them, the highest η value of 4.5% was obtained with **Mc[18,1]** dye. It was concluded that the distance between the chromophore and the TiO_2 surface

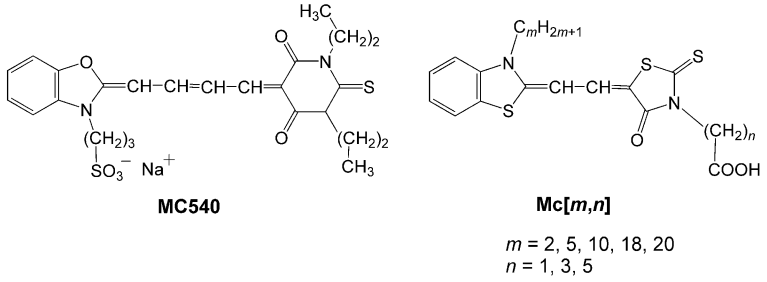

Figure 23. Molecular structures of merocyanine dye sensitizers.

affected the IPCE and that control of configuration and aggregation of the merocyanine dye is very important in improving solar cell efficiency.

3.6. Catechol Dyes

The DSSCs can be classified into two types: Type A and Type B, depending on the electron-injection pathway from the dye to the CB of the TiO_2.[79,80] The pathway for Type A is photoexcitation of the local band of the adsorbed dye followed by electron injection from the excited dye to the CB of the TiO_2. This pathway can also be called the "two-step" electron injection pathway. The dyes are bound to the surface of TiO_2 through carboxylic acid groups; Ru^{II} complexes, polyene dyes, coumarin dyes porphyrin dyes, and other dyes containing carboxylic acid groups have been known to inject electrons into TiO_2 according to the Type A pathway. The pathway for Type B, on the other hand, is direct, "one-step" electron injection from the ground state of the dye to the CB of the TiO_2 by photoexcitation of the dye-to-TiO_2 charge-transfer (DTCT) bands. Dyes containing enediol units have been known to bind to the TiO_2 surface through chelation of surface Ti^{IV} ions with the enediol groups, generally giving rise to very strong DTCT bands. In particular, catechol (**Cat**) dyes such as dopamine (**Dop**), fluorone, numerous natural pigments such as bromopyrogallol red (**Bpg**) and anthocyanins containing catechol moieties show strong DTCT bands in the visible region upon binding to TiO_2 (Figure 24).[81] However, dyes that belong to Type B have been hardly employed as sensitizers for DSSCs. The most serious problem for dyes of Type B until recently was that their η values had never exceeded 0.7%, because the back-electron-transfer rates from electrons injected into TiO_2 to the oxidized dye for pathway of Type B are faster than for the Type A pathway.

In an attempt to overcome this problem and to break through the η threshold of 0.7%, Yoon and co-workers found that attachment of electron-donating moieties such as (pyridin-4-yl)vinyl and (quinolin-4-yl)vinyl to **Cat** led to 2- and 2.7-fold increases, respectively, in η, driven by large increases in J_{sc}. As a result, the overall η values obtained with **Cat–v-P** and **Cat–v-Q** were 1.0% and 1.3%, respectively, breaking the 0.7% barrier for the first time.[80] The DSSCs based on **Cat–v-P** and **Cat–v-Q** clearly demonstrate that the attachment of a second donor group (pyridine or quinoline unit) to a primary donor (4-vinylcatechol unit) leads to a dramatic increase in electron injection efficiency. Yoon and co-workers proposed that both the consecutive charge shift from the secondary donor to a primary donor, leading to the retardation of back electron-transfer rate, and the red shift of the DTCT band caused by the increase in the donor strength of the dye through the attachment of the secondary donor to the primary donor were responsible for the increase in η.

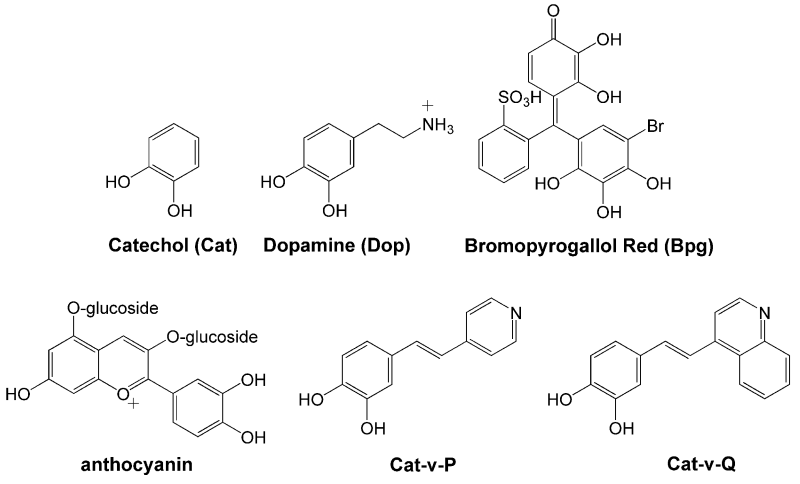

Figure 24. Molecular structures of catechol dye sensitizers.

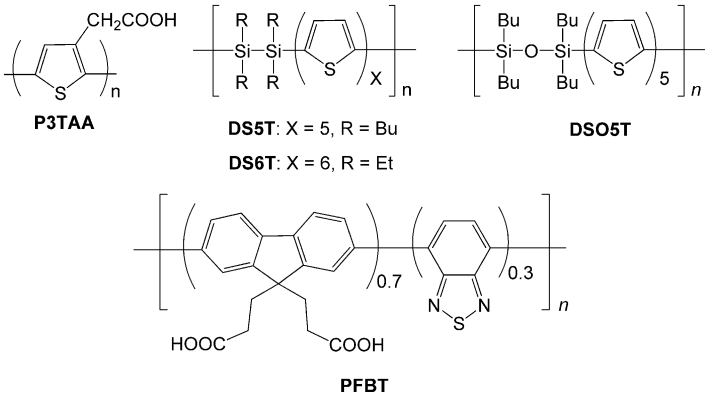

Figure 25. Molecular structures of polymeric dye sensitizers.

To improve the efficiency of DSSCs based on Type B catechol dyes further, the effective chemical modification of the catechol structure to retard back-electron-transfer is necessary and further study is desirable.

3.7. Polymeric Dyes

Recently, some efforts in the development of new dye sensitizers for DSSCs have focused on conjugated polymers such as polypyrrole, polyaniline, poly(*p*-phenyleneethynylene) and polythiophenes.[82–86] Conjugated polymers were reported to have large absorption coefficients and to permit fine-tuning of the HOMO and LUMO energy levels. Among them, polythiophenes are promising candidates as photosensitizers because of their thermal and environmental stabilities, conductivities, reversible transitions between redox and neutral states and potential for introduction of side chains to modify solubility and photophysical and electrochemical properties. A DSSCs based on poly(3-thiopheneacetic acid; **P3TAA**) shows $\eta \approx 1.6\%$ under 100 mW cm^{-2} irradiance (Figure 25).[85] Moreover, Yanagida et al. reported that the introduction of ionic liquids into electrolytes drastically enhanced the photovoltaic performances of the polythiophene-sensitized DSSC: $\eta \approx 2.4\%$, with $J_{sc} \approx 9.76$ mA cm^{-2}, $V_{oc} \approx 400$ mV, and *ff* of 0.61.[86]

On the other hand, an anionic conjugated polymer (**PFBT**) containing benzothiadiazole and polyfluorene as sensitizers was synthesized by Liu and Ramakrishna.[87] The absorption spectrum of **PFBT** covers the range from 280 to 510 nm, with the absorption maximum at 444 nm. The **PFBT**-sensitized solar cell gave a J_{sc} value of 4.03 mA cm^{-2}, a V_{oc} value of 523 mV and a *ff* value of 0.66, yielding an η value of 1.39% at AM1.5 (100 mW cm^{-2} light illumination).

More recently, Ohshita and Harima have reported interesting polymer-sensitized solar cells in which the attachment of disilanylene–oligothienylene alternate polymers (**DS5T**, **DS6T** and **DSO5T**, Figure 25) on TiO_2 surfaces is achieved by photochemical cleavage of the Si–Si bonds followed by formation of Ti–O–Si linkages between the polymers and the TiO_2 surface. When TiO_2 electrodes were dipped into chloroform solutions containing disilanylene–oligothienylene polymers and the solutions were irradiated ($\lambda_{max} > 400$ nm), polymer-bound electrodes that could be used for dye-sensitized solar cells were obtained.[88] The IPCE characteristics of DSSCs based on **DS5T** and **DS6T** showed clear sensitizing effects of polymers on the performance of the DSSCs: the maximum IPCE values for **DS5T** and **DS6T** were 10% at 460 nm and 15% at 490 nm, respectively. Although their photovoltaic performances were poor (η = 0.11 and 0.12% for **DS5T** and **DS6T**, respectively), this provides a novel method for preparation of polymer-bound TiO_2 electrodes that can be used for DSSCs.

To improve the efficiencies of DSSCs based on polymer dyes further, development of new polymeric dyes based on the accumulated molecular design strategy for organic dyes would be desirable.

3.8. Near-Infrared (NIR) Dyes

The organic dyes described above, such as coumarin dyes, polyene dyes, indoline dyes, porphyrin dyes and perylene dyes, exhibit relatively high DSSC performances, but these photosensitizers lack absorption in the red/NIR regions (600–1000 nm). To improve the performances of DSSCs further, it would be very useful to develop effective new NIR sensitizers for use in DSSCs, because red/NIR radiation (600–1000 nm) accounts for about 25% of the solar energy arriving on the Earth's surface [visible radiation (350–700 nm) accounts for about 45% of solar energy]. Unfortunately, there have until very recently been only a few reports on NIR sensitizers, such as squarylium dyes, phthalocyanine dyes, and cyanine dyes, with absorption maxima at around 700 nm, and the design and development of effective NIR sensitizers are therefore currently a hot topic in DSSC studies. The next subsections show the photovoltaic performances of DSSCs based on the squarylium dye, phthalocyanine dye and cyanine dye NIR sensitizers.

3.8.1. Squaraine Dyes

Squaraine dyes are well known for their intense absorption in the far-red/NIR, and as a result have been widely investigated as red/NIR sensitizers.[89–94] However, when

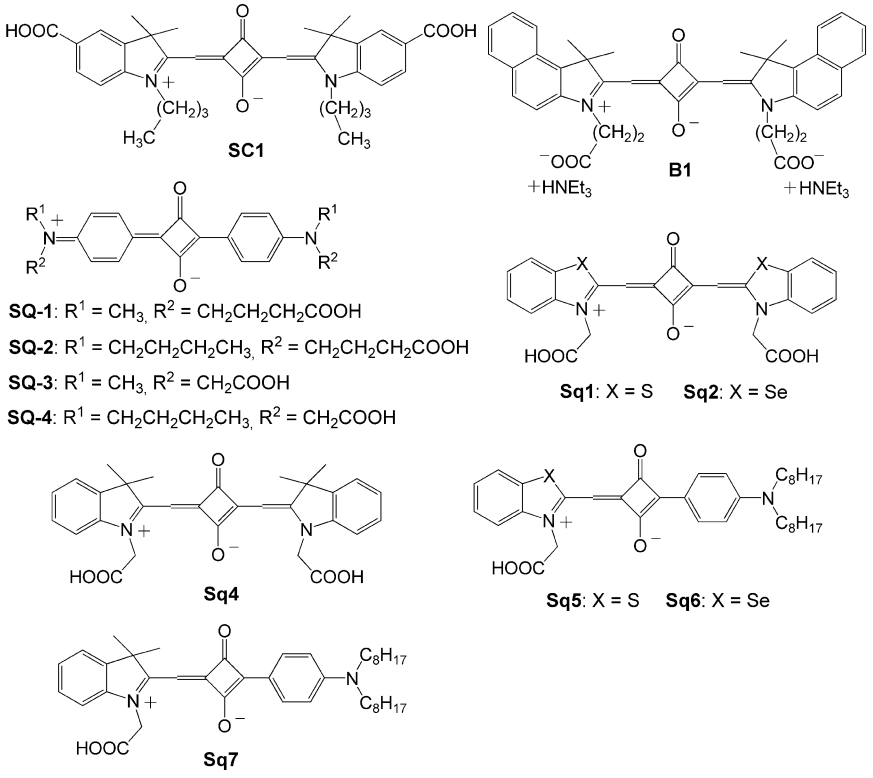

Figure 26. Molecular structures of squaraine dye sensitizers.

squaraine dyes were used in DSSCs, low IPCEs and η values were obtained. Squaraine dyes are well known easily to form H-aggregates (H-aggregates cause the blue shifts of the absorption bands relative to monomeric forms), which significantly affect their efficiency in DSSCs. Zhang and co-workers reported that a DSSC based on the symmetrical squaraine dye **SC1** gave an η value of 3.9% (Figure 26).[89] Furthermore, they reported four symmetrical squaraine dyes (**SQ1**–**SQ4**, λ_{max}^{abs} = 643–656 nm in DMSO) in DSSCs; those based on **SQ3** and **SQ4** gave η values of 3.2 and 3.4%, respectively.[90] In two reports they showed that the symmetrical squaraine dyes **SC1**, **SQ3** and **SQ4** formed H-aggregates on TiO_2 electrodes, which resulted in increases in their sensitization efficiencies in DSSCs.

In contrast, Palomares and co-workers directly addressed the role of the molecular aggregates in electron injection for a sensitized TiO_2 film.[91] The adsorption of a symmetrical squaraine dye on TiO_2 film resulted in a mixed population of aggregated and monomeric sensitizer dyes. They found that upon light excitation the electron injection only occurred from the monomers but that the yield remained high (ca. 95% of electrons are injected into the CB of the TiO_2) despite the presence of H-aggregates on the film. Recently, Grätzel and co-workers reported the highly efficient symmetrical squaraine dye **B1** (λ_{max}^{abs} = 679 nm, when adsorbed on TiO_2, Figure 26) incorporating two carboxylic acid attaching groups, which yielded an IPCE of 73% and an η value of 3.7% with J_{sc} = 8.6 mA cm^{-2}, V_{oc} = 591 mV and *ff* = 0.73 under AM 1.5G irradiation (100 mW cm^{-2}).[92] In order to prevent dye aggregation on the TiO_2 surface, chenodeoxycholic acid (CDCA) was used in the DSSCs based on **B1**.

On the other hand, a series of symmetrical (**Sq1**–**4**, λ_{max}^{abs} = 630–670 nm in solution, Figure 26) and unsymmetrical (**Sq5**–**7**, λ_{max}^{abs} = 600–630 nm in solution) squaraine dyes (the molecular structure of **Sq3** is the same as that of **SQ3**) have been synthesized, and their photovoltaic performances in DSSCs were evaluated by Das and co-workers. Unsymmetrical squaraine dyes exhibited much higher efficiencies as sensitizers than the symmetrical squaraine dyes.[93] Although the solar cell sensitized with the symmetrical squaraine **Sq1** gave an η value of 0.06%, the solar cell sensitized with the unsymmetrical squaraine **Sq5** gave an η value of 1.25%. The photovoltaic performances of the DSSCs based on these squaraine dyes are summarized in Table 6. They demonstrated that H-aggregation of symmetrical squaraine dyes on the TiO_2 photoelectrode resulted in significant decreases in their sensitization efficiencies, whereas efficient sensitization was observed from both the monomeric and H-aggregated forms of the unsymmetrical squaraine dyes. In addition, they suggested that a unidirectional flow of electrons toward the indoline moieties containing the carboxy anchoring groups on excitation of unsymmetrical squaraines could result in improved charge separation from the excited states of the symmetrical squaraines. This thus indicates that directionality of electrons in the excited state of a dye is one of the essential requirements for the development of an efficient squaraine sensitizer.

Table 6. Photovoltaic performances of DSSCs based on squaraine dyes **Sq1**–**7**.

Dye	J_{sc} [mA cm^{-2}]	V_{oc} [V]	*ff*	η (%)
Sq1	0.34	0.36	0.46	0.06
Sq2	0.32	0.42	0.52	0.07
Sq3	0.40	0.31	0.53	1.04
Sq4	3.52	0.53	0.53	1.25
Sq5	3.94	0.58	0.53	1.43
Sq6	3.78	0.60	0.61	2.08
Sq7	5.92	0.64	0.53	3.98

Recently, Nazeeruddin and co-workers proposed several basic requirements to guide the molecular engineering of efficient squaraine sensitizers.[94] 1) The excited-state redox potential of a dye should match the energy of the CB of the TiO_2 electrode (i.e., the LUMO level of the dye must be higher than the CB of the TiO_2 electrode). 2) Light excitation should be associated with vectorial electron flow from the light-harvesting moiety (chromophore) of the sensitizer towards the TiO_2 surface, providing for efficient electron transfer from the excited dye to the CB of the TiO_2 electrode. 3) Strong conjugation across the chromophore and anchoring groups is required for good electronic coupling between the LUMO of the dye and the CB of the TiO_2 electrode. In order to satisfy these requirements, they designed and developed the novel unsymmetrical squaraine sensitizer **DYE57** (Scheme 9), with a carboxylic acid group directly attached to the chromophore. The synthetic strategy used to obtain **DYE57** is shown in Scheme 9. In ethanol the squaraine **DYE57** shows an absorption maximum at 636 nm with high molar extinction coefficient (ε = 158500 dm^3 mol^{-1} cm^{-1}) corresponding to π–π* charge-transfer (CT) transitions. Under standard global AM 1.5 solar conditions, the solar cell sensitized with the unsymmetrical squaraine **DYE57** gave a J_{sc} value of 10.50 ± 0.20 mA cm^{-2}, a V_{oc} of 603 ± 30 mV and a *ff* of 0.71 ± 0.03, corresponding to an η value of 4.5%, which is the highest conversion efficiency so far reported for squaraine-based DSSCs. The IPCE was over 85%. They concluded that the high efficiency of **DYE57** was attributable to two particular molecular design features. Firstly, the carboxylic acid group is part of the conjugated π-system of the dye and provides strong electronic coupling to the CB of the TiO_2. Secondly, the asymmetry created by the octyl chain prevents surface aggregation and limits self-quenching of the excited state.

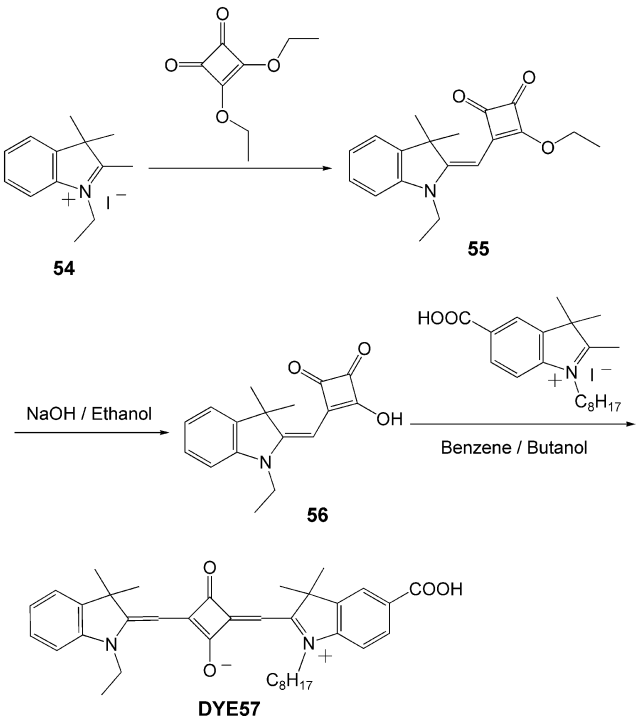

Scheme 9. Synthetic route to squaraine dye sensitizer **DYE57**.

As described above, however, there are differences in these reported results relating to the effects of H-aggregation on photovoltaic performances. For the design and development of more efficient squaraine dyes as photosensitizers, further fundamental study to obtain knowledge of their photoelectrochemical properties on TiO_2 electrodes is therefore necessary.

3.8.2. Cyanine Dyes

It is well known that cyanine dyes have very high absorption extinction coefficients (ca. 10^5 dm^3 mol^{-1} cm^{-1}), with intense and broad absorption bands in the visible and NIR. Recently, they have been used as sensitizers in DSSCs and some progress has been made in this area.[95–98] Cyanine dyes adsorbed on TiO_2 films can form J- or H-aggregates, which contribute to hypsochromism and bathochromism, respectively. It was found that J- and H-aggregated forms of these cyanine dyes sensitized with efficiencies equal to those of the monomer forms.[95] On the other hand, in order to find a guiding principle for designing efficient cyanine dye sensitizers, Arakawa and co-workers systematically investigated the photoelectrochemical properties of TiO_2 electrodes sensitized with the various cyanine dyes **Cn-D** (n = 0–3), **Cn-N** (n = 1–3), **C1′**, **C1-D#**, **C2-Ns** and **C2-ND** with different anchoring groups (Figure 27).[96] They found that the distance between the cyanine skeleton and TiO_2 surface significantly influenced the photocurrent efficiency: the IPCEs of the cyanine dye-sensitized solar cells increased with decreasing distance between the dye skeletons and the TiO_2 surface, due to efficient charge transfer between them. The IPCE of **C1-D** is thus about twice as large as those of **C1-N** and **C1-D#**. In addition, they found that although the absorption maxima shift to longer wavelength by ca. 100 nm with each increase of one methine unit (n), the increasing lengths of the methine chains in the dyes enhanced the difficulty of electron transfer from the excited dyes to the CB of the TiO_2, so that the IPCE dramatically decreased with increasing numbers of methine units (n). It was suggested further that the positive shift in the dye potential (the LUMO level) in the excited state with increasing methine units (n) was the main reason for the decrease in the IPCE. Therefore, it was also concluded for cyanine dyes that the photocurrent is governed by the relationship be-

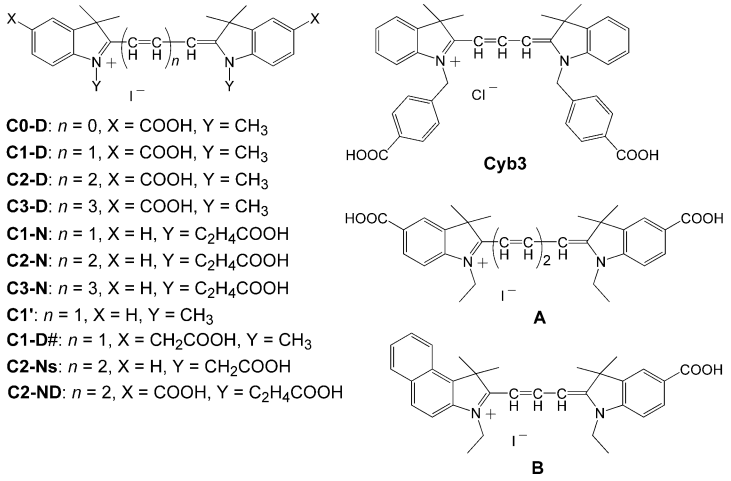

Figure 27. Molecular structures of symmetrical cyanine dye sensitizers.

tween the potentials of the excited dye and the CB of the TiO_2 electrode. Out of these, the highest η value was obtained with **C1-D**.

Cai and co-workers recently synthesized the new symmetrical cyanine dyes **Cyb3** and **A** and the unsymmetrical cyanine dye **B** as sensitizers for DSSCs (Figure 27). They found that the aggregates of the cyanine dyes were efficient in light harvesting, and the DSSCs based on **Cyb3**, **A** and **B** gave η values of 1.01, 1.3, and 2.9%, respectively.[97] Thus, for a variety of cyanine dyes, structurally asymmetric ones exhibit more outstanding performances. Unlike in symmetric cyanine dyes, the shifts in electron density in their unsymmetrical counterparts occur towards the indole ring containing the carboxylic acid group used for linking the molecule to the TiO_2 surface. A unidirectional flow of electron distribution can result in favourable charge separation and electron injection in a DSSC. Accordingly, Tian and co-workers have more recently synthesized the unsymmetrical cyanine dyes **Cy1**, **Cy2** and **Cy3** with different alkyl chain lengths between the naphthalimide and triazole groups as sensitizers for DSSCs, and have systematically investigated the relationship between the photoelectrochemical properties and structures.[98] The synthetic route is shown in Scheme 10. The absorption peaks of **Cy1**–**Cy3** in solution are at 550 and 583 nm for **Cy1**, 408, 550 and 583 nm for **Cy2** and 408, 550 and 583 nm for **Cy3**. Interestingly, these cyanine dyes adsorbed on TiO_2 film can form J- or H-aggregates, which broaden the absorption spectra to both red and blue sides and which should in turn enhance the conversion efficiency of light into electricity. In

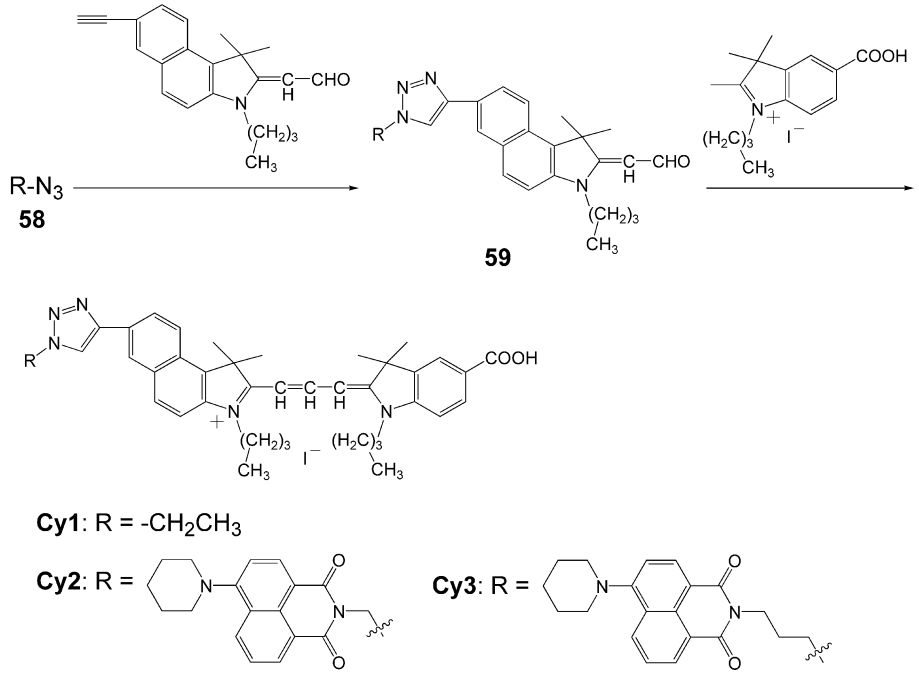

Scheme 10. Synthetic route to unsymmetrical cyanine dye sensitizers **Cy1**–**3**.

addition, for **Cy2** and **Cy3**, the J_{sc} and V_{oc} values increased with increasing alkyl chain length between the naphthalimide and triazole groups; consequently, the η value also increased with increasing alkyl chain length. An increase in alkyl chain length might be expected to prevent the recombination processes of injected electrons with dye cations and with I_3^- ions in the electrolyte. Of the three cyanine dyes, it was found that **Cy3** generated the highest η value of 4.80%.

3.8.3. Phthalocyanine Dyes

Phthalocyanines (**Pc**s) are typical NIR dyes in terms of their intense absorptions in the UV/blue (Soret band) and the red/NIR (Q band at around 700 nm) spectral regions, as well as of their electrochemical, photochemical and thermal stabilities. They are therefore attractive as sensitizer dyes for DSSCs. Several groups have tested phthalocyanines as sensitizers for TiO_2 electrodes, although until recently they had all have reported η values around 1%.[99] Grätzel and co-workers reported a high IPCE of 45% in the NIR for DSSCs based on a (2,9,16,23-tetracarboxyphthalocyaninato)zinc(II)-sensitized (**ZnTcPc**-sensitized) TiO_2 electrode, which showed an η value of 1.0% (Figure 28).[100] The low efficiencies of DSSCs incorporating phthalocyanines appear to be due to aggregation, lack of directionality in the excited state and poor electronic coupling between the phthalocyanine LUMO and the CB of the TiO_2. Introduction of bulky substituents – *tert*-butyl groups or tyrosine groups – into the phthalocyanine skeleton serves not only to minimize the formation of molecular aggregates, but also to enhance solubility in organic solvents.[101]

Recently, to overcome the drawbacks described above, Grätzel and Nazeeruddin designed and developed a novel unsymmetrical phthalocyaninatozinc (**PCH001**) sensitizer (Scheme 11) containing three *tert*-butyl and two carboxylic acid groups that act as "push" and "pull" groups, respectively, which not only provides efficient electron transfer from the excited dye to the TiO_2 electrode through good electronic coupling between the LUMO of the dye and the CB level of the TiO_2, but also minimizes the formation of molecular aggregates.[102] Scheme 11 shows the synthetic strategy used for the preparation of phthalocyanine sensitizer **PCH001**. The push-pull character induces directionality in the excited state of the phthalocyaninatozinc. Again, the purposes of the three *tert*-butyl groups are to enhance the solubility, to minimize the aggregation and to tune the LUMO level of the phthalocyanine to provide directionality in the excited state. The functions of the two carboxylic acid groups are to attach the sensitizer on the TiO_2 surface and to provide intimate electronic coupling between the excited dye and the CB of the TiO_2 electrode. A **PCH001**-sensitized solar cell gave a J_{sc} value of 6.50 ± 0.20 mA cm^{-2}, V_{oc} of 635 ± 30 mV and *ff* of 0.74 ± 0.03, corresponding to an η value of 3.05% under standard global air mass (AM) 1.5 solar conditions.

The same workers also synthesized the new phthalocyaninatozinc sensitizer **TT1** (Figure 28).[103] The visible absorption spectrum of **TT1** on TiO_2 shows a maximum at

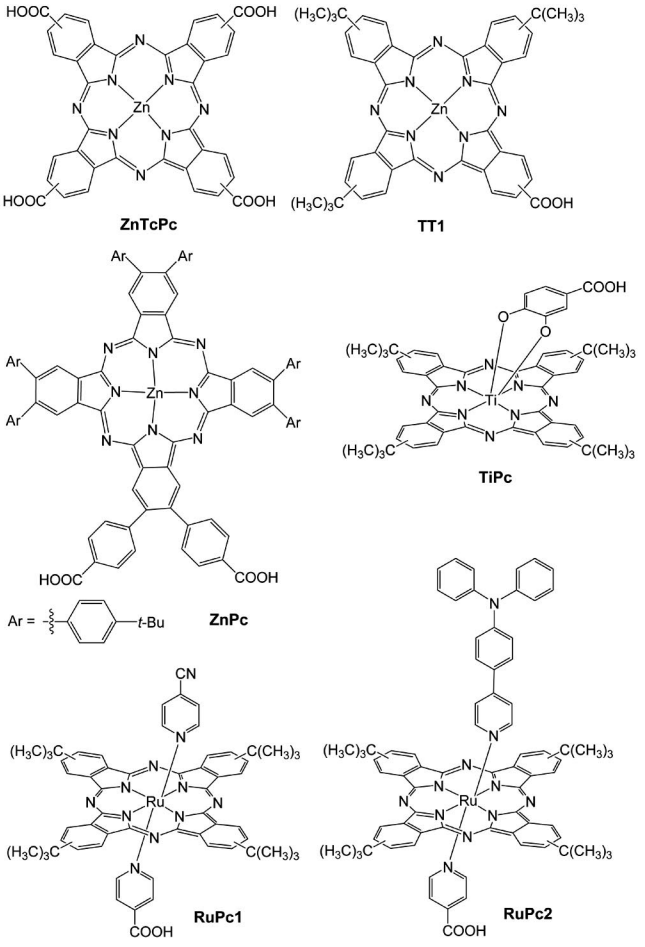

Figure 28. Molecular structures of phthalocyanine dye sensitizers.

680 nm, which is in good agreement with that of the **TT1** in solution and implies a low degree of molecular aggregation on the TiO_2 surface. A DSSC based on **TT1** showed impressive efficiency under simulated solar irradiation conditions (1 sun = 100 mW cm^{-2} 1.5 air mass global) of 3.52% with $J_{sc} = 7.60 \pm 0.20$ mA cm^{-2}, $V_{oc} = 617 \pm 20$ mV and *ff* $= 0.75 \pm 0.02$. This is the highest efficiency ever reported for a phthalocyaninatozinc DSSC. The IPCE at the maximum absorption of the Q band reaches 80%.

On the other hand, Durrant and co-workers reported that novel Ru- (**RuPc1** and **RuPc2**) and Ti-phthalocyanine dye (**TiPc**) sensitizers (Figure 28) with axial ligands have strong photo-absorption properties in the red region and that their axial ligands not only anchor the dye to TiO_2 surface, but also hinder the formation of aggregates.[104] On the other hand, Imahori and co-workers reported the synthesis and photovoltaic properties of the novel highly substituted zinc complex with phthalocyaninecarboxylic acid **ZnPc** with eight sterically hindered 4-*tert*-butylphenyl groups, which displayed high solubility in common organic solvents and a reduced tendency towards dye aggregation.[105]

However, the power conversion efficiencies of phthalocyanine-based DSSCs are much lower than those of other organic dye-based DSSCs. Further studies to elucidate the

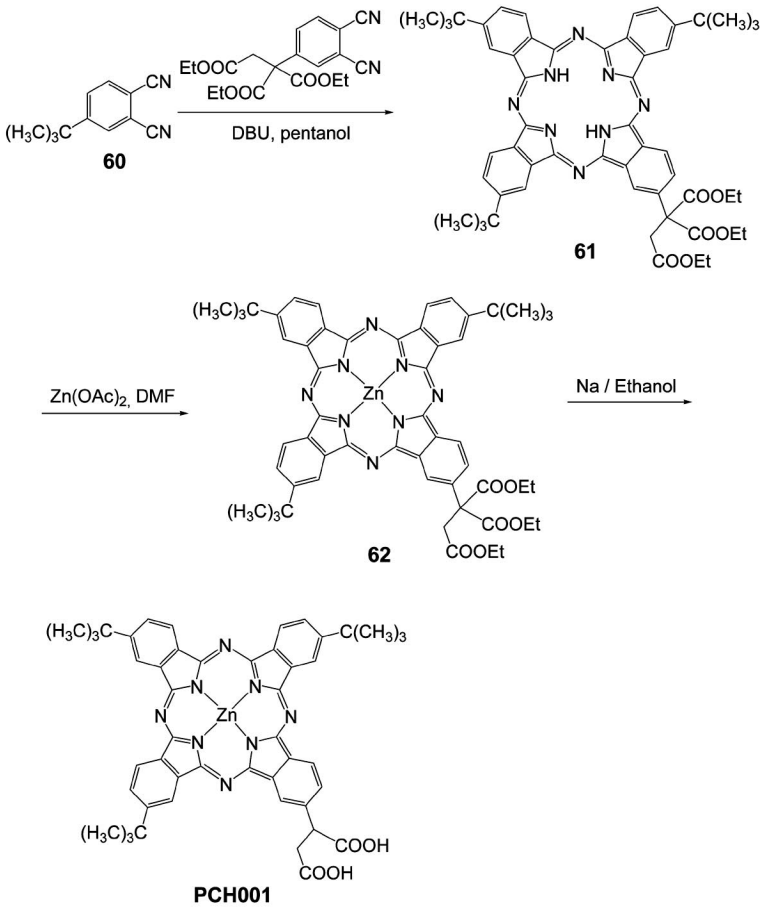

Scheme 11. Synthetic route to phthalocyanine dye sensitizer **PCH001**.

close relationship between molecular structure and photovoltaic properties for the improvement of the performances of DSSCs based on phthalocyanine sensitizers are still needed.

4. Conclusions

During the last decade, much effort has been made on the development of various types of organic dye sensitizers for DSSCs, and there has been a gradual accumulation of information about the relationship between the chemical structures and photovoltaic performances of DSSCs. DSSCs based on organic dyes have reached η values as high as 9%, comparable to those of Ru complexes (η = 10–11%). The η values of DSSCs based on the organic dyes mentioned in this microreview are as follows: coumarines (up to 7.7%), polyenes (up to 7.0%), hemicyanines (up to 5.2%), thiophenes (up to 8.6%), indolines (up to 9.5%), heteropolycyclics (up to 1.5%), xanthenes (up to <1%), perylenes (up to 6.6%), porphyrins (up to 7.1%), merocyanines (up to 4.5%), catechols (up to 1.3%), polymers (up to 2.4%), squaraines (up to 4%), cyanines (up to 4.8%) and phthalocyanines (up to 3.5%). Out of these organic dye sensitizers, D-π-A dyes possessing broad and intense absorption spectral features in the visible region have exhibited especially excellent performances and are regarded as one of the most promising classes of organic sensitizers. Recently, NIR dye sensitizers providing good absorption in the red/NIR region of the solar spectrum have attracted increasing interest. Therefore, a successful strategy to improve performances of DSSCs is to develop panchromatic organic sensitizers possessing broad absorption characteristics extending throughout the visible and NIR regions. Breakthroughs in novel molecular design and synthetic strategy would be expected to be achieved by organic chemists.

Acknowledgments

Very special thanks are due to the current and former members of our research group for the most valuable contributions to our work on dye-sensitized solar cells. Grants-in-Aid from The Japan Society for the Promotion of Science (JSPS) for Scientific Research (B) (19350094) and for Young Scientists (B) (20750161), and from the Electric Technology Research Foundation of Chugoku are gratefully acknowledged.

[1] M. Grätzel, *Nature* **2001**, *414*, 338–344.
[2] A. Hagfeldt, M. Grätzel, *Chem. Rev.* **1995**, *95*, 49–68.
[3] U. Bach, D. Lupo, P. Comte, J. E. Moser, F. Weissörtel, J. Salbeck, H. Spreitzer, M. Grätzel, *Nature* **1998**, *395*, 583–585.

[4] M. K. Nazeeruddin, S. M. Zakeeruddin, J.-J. Lagref, P. Liska, P. Comte, C. Barolo, G. Viscardi, K. Schenk, M. Grätzel, *Coord. Chem. Rev.* **2004**, *248*, 1317–1328.
[5] A. S. Polo, M. K. Itokazu, N. Y. M. Iha, *Coord. Chem. Rev.* **2004**, *248*, 1343–1361.
[6] M. Grätzel, *Inorg. Chem.* **2005**, *44*, 6841–6851.
[7] S. Nakade, T. Kanzaki, W. Kubo, T. Kitamura, Y. Wada, S. Yanagida, *J. Phys. Chem. B* **2005**, *109*, 3480–3487.
[8] N. Robertson, *Angew. Chem. Int. Ed.* **2006**, *45*, 2338–2345.
[9] J. R. Durrant, S. A. Haque, E. Palomares, *Chem. Commun.* **2006**, 3279–3289.
[10] L. M. Peter, *Phys. Chem. Chem. Phys.* **2007**, *9*, 2630–2642.
[11] K. R. Millington, K. W. Fincher, A. L. King, *Sol. Energy Mater. Sol. Cells* **2007**, *91*, 1618–1630.
[12] P. Xie, F. Guo, *Curr. Org. Chem.* **2007**, *11*, 1272–1286.
[13] Z. Chen, F. Li, C. Huang, *Curr. Org. Chem.* **2007**, *11*, 1241–1258.
[14] N. Robertson, *Angew. Chem. Int. Ed.* **2008**, *47*, 1012–1014.
[15] A. B. F. Martinson, T. W. Hamann, M. J. Pellin, J. T. Hupp, *Chem. Eur. J.* **2008**, *14*, 4458–4467.
[16] B. O'Regan, M. Grätzel, *Nature* **1991**, *353*, 737–740.
[17] M. K. Nazeeruddin, A. Kay, I. Rodicio, R. Humphry-Baker, E. Müller, P. Liska, N. Vlachopolous, M. Grätzel, *J. Am. Chem. Soc.* **1993**, *115*, 6382–6390.
[18] a) M. K. Nazeeruddin, P. Pechy, *Chem. Commun.* **1997**, 1705–1706; b) M. K. Nazeeruddin, P. Pechy, T. Renouard, S. M. Zakeeruddin, R. Humphry-Baker, P. Comte, P. Liska, L. Cevey, E. Costa, V. Shklover, L. Spiccia, G. B. Deacon, C. A. Bignozzi, M. Grätzel, *J. Am. Chem. Soc.* **2001**, *123*, 1613–1624.
[19] a) K. Hara, K. Sayama, Y. Ohga, A. Shinpo, S. Suga, H. Arakawa, *Chem. Commun.* **2001**, 569–570; b) K. Hara, Y. Tachibana, Y. Ohga, A. Shinpo, S. Suga, K. Sayama, H. Sugihara, H. Arakawa, *Sol. Energy Mater. Sol. Cells* **2003**, *77*, 89–103; c) K. Hara, T. Sato, R. Katoh, A. Furude, Y. Ohga, A. Shinpo, S. Suga, K. Sayama, H. Sugihara, H. Arakawa, *J. Phys. Chem. B* **2003**, *107*, 597–606; d) A. Furube, R. Katoh, K. Hara, T. Sato, S. Murata, H. Arakawa, M. Tachiya, *J. Phys. Chem. B* **2005**, *109*, 16406–16414.
[20] a) K. Hara, M. Kurashige, Y. Dan-oh, C. Kasada, A. Shinpo, S. Suga, K. Sayama, H. Arakawa, *New J. Chem.* **2003**, *27*, 783–785; b) K. Hara, Y. Dan-oh, C. Kasada, Y. Ohga, A. Shinpo, S. Suga, K. Sayama, H. Arakawa, *Langmuir* **2004**, *20*, 4205–4210; c) K. Hara, Z.-S. Wang, T. Sato, A. Furube, R. Katoh, H. Sugihara, Y. Dan-oh, C. Kasada, A. Shinpo, S. Suga, *J. Phys. Chem. B* **2005**, *109*, 15476–15482; d) K. Hara, K. Miyamoto, Y. Abe, M. Yanagida, *J. Phys. Chem. B* **2005**, *109*, 23776–23778.
[21] a) Z.-S. Wang, Y. Cui, K. Hara, Y. Dan-oh, C. Kasada, A. Shinpo, *Adv. Mater.* **2007**, *19*, 1138–1141; b) Z.-S. Wang, Y. Cui, Y. Dan-oh, C. Kasada, A. Shinpo, K. Hara, *J. Phys. Chem. C* **2008**, *112*, 17011–17017.
[22] Z.-S. Wang, K. Hara, Y. Dan-oh, C. Kasada, A. Shinpo, S. Suga, H. Arakawa, H. Sugihara, *J. Phys. Chem. B* **2005**, *109*, 3907–3914.
[23] Z.-S. Wang, Y. Cui, Y. Dan-oh, C. Kasada, A. Shinpo, K. Hara, *J. Phys. Chem. C* **2007**, *111*, 7224–7230.
[24] a) K. Hara, M. Kurashige, S. Ito, A. Shinpo, S. Suga, K. Sayama, H. Arakawa, *Chem. Commun.* **2003**, 252–253; b) K. Hara, T. Sato, R. Katoh, A. Furube, T. Yoshihara, M. Murai, M. Kurashige, S. Ito, A. Shinpo, S. Suga, H. Arakawa, *Adv. Funct. Mater.* **2005**, *15*, 246–252.
[25] a) D. P. Hagberg, T. Edvinsson, T. Marinado, G. Boschloo, A. Hagfeldt, L. Sun, *Chem. Commun.* **2006**, 2245–2247; b) E. M. J. Johansson, T. Edvinsson, M. Odelius, D. P. Hagberg, L. Sun, A. Hagfeld, H. Siegbahn, H. Rensmo, *J. Phys. Chem. C* **2007**, *111*, 8580–8586; c) D. P. Hagberg, T. Marinado, K. M. Karlsson, K. Nonomura, P. Qin, G. Boschloo, T. Brinck, A. Hagfeldt, L. Sun, *J. Org. Chem.* **2007**, *72*, 9550–9556; d) D. P. Hagberg, J.-H. Yum, H. Lee, F. D. Angelis, T. Marinado, K. M. Karlsson, R. Humphry-Baker, L. Sun, A. Hagfeldt, M. Grätzel, M. K. Nazeeruddin, *J. Am. Chem. Soc.* **2008**, *130*, 6259–6266.
[26] H. Tian, X. Yang, R. Chen, R. Zhang, A. Hagfeldt, L. Sun, *J. Phys. Chem. C* **2008**, *112*, 11023–11033.
[27] C. Kim, H. Choi, S. Kim, C. Baik, K. Song, M.-S. Kang, S. O. Kang, J. Ko, *J. Org. Chem.* **2008**, *73*, 7072–7079.
[28] a) I. Jung, J. K. Lee, K. H. Song, K. Song, S. O. Kang, J. Ko, *J. Org. Chem.* **2007**, *72*, 3652–3658; b) D. Kim, J. K. Lee, S. O. Kang, J. Ko, *Tetrahedron* **2007**, *63*, 1913–1922; c) H. Choi, J. K. Lee, K. Song, S. O. Kang, J. Ko, *Tetrahedron* **2007**, *63*, 3115–3121; d) S. Kim, H. Choi, D. Kim, K. Song, S. O. Kang, J. Ko, *Tetrahedron* **2007**, *63*, 9206–9212; e) S. Kim, H. Choi, C. Baik, K. Song, S. O. Kang, J. Ko, *Tetrahedron* **2007**, *63*, 11436–11443.
[29] a) K. R. J. Thomas, J. T. Lin, Y.-C. Hsu, K.-C. Ho, *Chem. Commun.* **2008**, 4098–4100; b) Y.-S. Yen, Y.-C. Hsu, J. T. Lin, C.-W. Chang, C.-P. Hsu, D.-J. Yin, *J. Phys. Chem. C* **2008**, *112*, 12557–12567.
[30] G. Zhou, N. Pschirer, J. C. Schöneboom, F. Eickemeyer, M. Baumgarten, K. Müllen, *Chem. Mater.* **2008**, *20*, 1808–1815.
[31] a) T. Kitamura, M. Ikeda, K. Shigaki, T. Inoue, N. A. Anderson, X. Ai, T. Lian, S. Yanagida, *Chem. Mater.* **2004**, *16*, 1806–1812; b) Y. Chen, C. Li, Z. Zeng, W. Wang, X. Wang, B. Zhang, *Chem. Lett.* **2005**, *34*, 762–763; c) X.-F. Wang, Y. Koyama, H. Nagae, Y. Yamano, M. Ito, Y. Wada, *Chem. Phys. Lett.* **2006**, *420*, 309–315; d) S. Hwang, J. H. Lee, C. Park, H. Lee, C. Kim, C. Park, M.-H. Lee, W. Lee, J. Park, K. Kim, N.-G. Park, C. Kim, *Chem. Commun.* **2007**, 4887–4889; e) M. Liang, W. Xu, F. Cai, P. Chen, B. Peng, J. Chen, Z. Li, *J. Phys. Chem. C* **2007**, *111*, 4465–4472; f) W. Xu, J. Pei, J. Shi, S. Peng, J. Chen, *J. Power Sources* **2008**, *183*, 792–798; g) W. Xu, B. Peng, J. Chen, M. Liang, F. Cai, *J. Phys. Chem. C* **2008**, *112*, 874–880; h) Z. Ning, Q. Zhang, W. Wu, H. Pei, B. Liu, H. Tian, *J. Org. Chem.* **2008**, *73*, 3791–3797.
[32] a) M. Velusamy, K. R. J. Thomas, J. T. Lin, Y.-C. Hsu, K.-C. Ho, *Org. Lett.* **2005**, *7*, 1899–1902; b) S.-L. Li, K.-J. Jiang, K.-F. Shao, L.-M. Yang, *Chem. Commun.* **2006**, 2792–2794; c) R. Chen, X. Yang, H. Tian, L. Sun, *J. Photochem. Photobiol. A: Chem.* **2007**, *189*, 295–300; d) P. Qin, X. Yang, R. Chen, L. Sun, *J. Phys. Chem. C* **2007**, *111*, 1853–1860; e) H. Tian, X. Yang, R. Chen, Y. Pan, L. Li, A. Hagfeldt, L. Sun, *Chem. Commun.* **2007**, 3741–3743; f) G. Li, K.-J. Jiang, Y.-F. Li, S.-L. Li, L.-M. Yang, *J. Phys. Chem. C* **2008**, *112*, 11591–11599.
[33] Z.-S. Wang, F.-Y. Li, C.-H. Huang, L. Wang, M. Wei, L.-P. Jin, N.-Q. Li, *J. Phys. Chem. B* **2000**, *104*, 9676–9682.
[34] Y.-S. Chen, C. Li, Z.-H. Zeng, W.-B. Wang, X.-S. Wang, B.-W. Zhang, *J. Mater. Chem.* **2005**, *15*, 1654–1661.
[35] Q.-H. Yao, F.-S. Meng, F.-Y. Li, H. Tian, C.-H. Huang, *J. Mater. Chem.* **2003**, *13*, 1048–1053.
[36] a) Z.-S. Wang, F.-Y. Li, C.-H. Huang, *Chem. Commun.* **2000**, 2063–2064; b) Z.-S. Wang, F.-Y. Li, C.-H. Huang, *J. Phys. Chem. B* **2001**, *105*, 9210–9217; c) Q.-H. Yao, L. Shan, F.-Y. Li, D.-D. Yin, C.-H. Huang, *New J. Chem.* **2003**, *27*, 1277–1283.
[37] a) E. Stathatos, P. Lianos, A. Laschewsky, O. Ouari, P. Van Cleuvenbergen, *Chem. Mater.* **2001**, *13*, 3888–3892; b) F. S. Meng, Q. H. Yao, J. G. Shen, F. L. Li, C. H. Huang, K. C. Chen, H. Tian, *Synth. Met.* **2003**, *137*, 1543–1544.
[38] K. Tanaka, K. Takimiya, T. Otsubo, K. Kawabuchi, S. Kajihara, Y. Harima, *Chem. Lett.* **2006**, *35*, 592–593.
[39] S. Tan, J. Zhai, H. Fang, T. Jiu, J. Ge, Y. Li, L. Jiang, D. Zhu, *Chem. Eur. J.* **2005**, *11*, 6272–6276.
[40] a) N. Koumura, Z.-S. Wang, S. Mori, M. Miyashita, E. Suzuki, K. Hara, *J. Am. Chem. Soc.* **2006**, *128*, 14256–14257; b) Z.-S. Wang, N. Koumura, Y. Cui, M. Takahashi, H. Sekiguchi, A. Mori, T. Kubo, A. Furube, K. Hara, *Chem. Mater.* **2008**, *20*, 3993–4003.
[41] H. Choi, C. Baik, S. O. Kang, J. Ko, M.-S. Kang, M. K. Nazeeruddin, M. Grätzel, *Angew. Chem. Int. Ed.* **2008**, *47*, 327–330.

[42] S. Kim, D. Kim, H. Choi, M.-S. Kang, K. Song, S. O. Kang, J. Ko, *Chem. Commun.* **2008**, 4951–4953.

[43] a) S. Kim, J. K. Lee, S. O. Kang, J. Ko, J.-H. Yum, S. Frantacci, F. D. Angelis, D. D. Censo, M. K. Nazeeruddin, M. Grätzel, *J. Am. Chem. Soc.* **2006**, *128*, 16701–16707; b) H. Choi, J. K. Lee, K. H. Song, K. Song, S. O. Kang, J. Ko, *Tetrahedron* **2007**, *63*, 1553–1559; c) D. Kim, M.-S. Kang, K. Song, S. O. Kang, J. Ko, *Tetrahedron* **2008**, *64*, 10417–10424.

[44] W.-H. Liu, I.-C. Wu, C.-H. Lai, C.-H. Lai, P.-T. Chou, Y.-T. Li, C.-L. Chen, Y.-Y. Hsu, Y. Chi, *Chem. Commun.* **2008**, 5152–5154.

[45] K. R. J. Thomas, Y.-C. Hsu, J. T. Lin, K.-M. Lee, K.-C. Ho, C.-H. Lai, Y.-M. Cheng, P.-T. Chou, *Chem. Mater.* **2008**, *20*, 1830–1840.

[46] H. Qin, S. Wenger, M. Xu, F. Gao, X. Jing, P. Wang, S. M. Zakeeruddin, M. Grätzel, *J. Am. Chem. Soc.* **2008**, *130*, 9202–9203.

[47] a) M.-S. Tsai, Y.-C. Hsu, J. T. Lin, H.-C. Chen, C.-P. Hsu, *J. Phys. Chem. C* **2007**, *111*, 18785–18793; b) R. Chen, X. Yang, H. Tian, X. Wang, A. Hagfeldt, L. Sun, *Chem. Mater.* **2007**, *19*, 4007–4015.

[48] a) T. Horiuchi, H. Miura, S. Uchida, *Chem. Commun.* **2003**, 3036–3037; b) T. Horiuchi, H. Miura, S. Uchida, *J. Photochem. Photobiol. A: Chem.* **2004**, *164*, 29–32; c) T. Horiuchi, H. Miura, K. Sumioka, S. Uchida, *J. Am. Chem. Soc.* **2004**, *126*, 12218–12219; d) L. Schmidt-Mende, U. Bach, R. Humphry-Baker, T. Horiuchi, H. Miura, S. Ito, S. Uchida, M. Grätzel, *Adv. Mater.* **2005**, *17*, 813–815; e) S. Ito, S. M. Zakeeruddin, R. Humphry-Baker, P. Liska, R. Charvet, P. Comte, M. K. Nazeeruddin, P. Péchy, M. Takata, H. Miura, S. Uchida, M. Grätzel, *Adv. Mater.* **2006**, *18*, 1202–1205; f) W. H. Howie, F. Claeyssens, H. Miura, L. M. Peter, *J. Am. Chem. Soc.* **2008**, *130*, 1367–1375.

[49] a) D. Kuang, S. Uchida, R. Humphry-Baker, S. K. Zakeeruddin, M. Grätzel, *Angew. Chem. Int. Ed.* **2008**, *47*, 1923–1927; b) S. Ito, H. Miura, S. Uchida, M. Takata, K. Sumioka, P. Liska, P. Comte, P. Péchy, M. Grätzel, *Chem. Commun.* **2008**, 5194–5196.

[50] Y. Ooyama, Y. Shimada, Y. Kagawa, I. Imae, Y. Harima, *Org. Biomol. Chem.* **2007**, *5*, 2046–2054.

[51] a) Y. Ooyama, Y. Shimada, Y. Kagawa, Y. Yamada, I. Imae, K. Komaguchi, Y. Harima, *Tetrahedron Lett.* **2007**, *48*, 9167–9170; b) Y. Ooyama, Y. Shimada, A. Ishii, G. Ito, Yu. Kagawa, I. Imae, K. Komaguchi, Y. Harima, *J. Photochem. Photobiol. A* **2009**, *203*, 177–185.

[52] a) Y. Ooyama, Y. Harima, *Chem. Lett.* **2006**, *8*, 902–903; b) Y. Ooyama, Y. Kagawa, Y. Harima, *Eur. J. Org. Chem.* **2007**, 3613–3621; c) Y. Ooyama, A. Ishii, Y. Kagawa, I. Imae, Y. Harima, *New J. Chem.* **2007**, *31*, 2076–2082.

[53] K. Sayama, M. Sugino, H. Sugihara, Y. Abe, H. Arakawa, *Chem. Lett.* **1998**, *27*, 753–754.

[54] K. Hara, T. Horiguchi, T. Kinoshita, K. Sayama, H. Sugihara, H. Arakawa, *Sol. Energy Mater. Sol. Cells* **2000**, *64*, 115–134.

[55] S. Hattori, T. Hasobe, K. Ohkubo, Y. Urano, N. Umezawa, T. Nagano, Y. Wada, S. Yanagida, S. Fukuzumi, *J. Phys. Chem. B* **2004**, *108*, 15200–15205.

[56] J. R. Mann, M. K. Gannon, T. C. Fitzgibbons, M. R. Detty, D. F. Watson, *J. Phys. Chem. C* **2008**, *112*, 13057–13061.

[57] a) M. K. I. Senevirathna, P. K. D. D. P. Pitigala, K. Tennakone, *J. Phys. Chem. B* **2005**, *109*, 16030–16033; b) M. S. Roy, P. Balraju, M. Kumar, G. D. Sharma, *Sol. Energy Mater. Sol. Cells* **2008**, *92*, 909–913.

[58] a) S. Ferrere, B. A. Gregg, *J. Phys. Chem. B* **2001**, *105*, 7602–7605; b) S. Ferrere, B. A. Gregg, *New J. Chem.* **2002**, *26*, 1155–1160.

[59] T. Edvinsson, C. Li, N. Pschirer, J. Schöneboom, F. Eickemeyer, R. Sens, G. Boschloo, A. Herrmann, K. Müllen, A. Hagfeldt, *J. Phys. Chem. C* **2007**, *111*, 15137–15140.

[60] C. Li, J.-H. Yum, S.-J. Moon, A. Herrmann, F. Eickemeyer, N. G. Pschirer, P. Erk, J. Schöneboom, K. Müllen, M. Grätzel, M. K. Nazeeruddin, *ChemSusChem* **2008**, *1*, 615–618.

[61] a) S. Ferrere, A. Zaban, B. A. Gregg, *J. Phys. Chem. B* **1997**, *101*, 4490–4493; b) C. Zafer, M. Kus, G. Turkmen, H. Dincalp, S. Demic, B. Kuban, Y. Teoman, S. Icli, *Sol. Energy Mater. Sol. Cells* **2007**, *91*, 427–431; c) J. Fortage, M. Séverac, C. Houarner-Rassin, Y. Pellegrin, E. Blart, F. Odobel, *J. Photochem. Photobiol. A: Chem.* **2008**, *197*, 156–169; d) Y. Jin, J. Hua, W. Wu, X. Ma, F. Meng, *Synth. Met.* **2008**, *158*, 64–71.

[62] Y. Shibano, T. Umeyama, Y. Matano, H. Imahori, *Org. Lett.* **2007**, *9*, 1971–1974.

[63] A. Kay, M. Grätzel, *J. Phys. Chem.* **1993**, *97*, 6272–6277.

[64] a) X.-F. Wang, C.-H. Zhan, T. Maoka, Y. Wada, Y. Koyama, *Chem. Phys. Lett.* **2007**, *447*, 79–85; b) X.-F. Wang, Y. Koyama, H. Nagae, Y. Wada, S. Sasaki, H. Tamiaki, *J. Phys. Chem. B* **2008**, *112*, 4418–4426.

[65] S. Cherian, C. C. Wamser, *J. Phys. Chem. B* **2000**, *104*, 3624–3629.

[66] Y. Tachibana, S. A. Haque, I. P. Mereer, J. R. Durrant, D. R. Klug, *J. Phys. Chem. B* **2000**, *104*, 1198–1205.

[67] A. Forneli, M. Olanells, M. A. Sarmentero, E. Matyinez-Ferrero, B. C. O'Regan, P. Ballester, E. Palomares, *J. Mater. Chem.* **2008**, *18*, 1652–1658.

[68] M. Gervaldo, F. Fungo, E. N. Durantini, J. J. Silber, L. Sereno, L. Otero, *J. Phys. Chem. B* **2005**, *109*, 20953–20962.

[69] M. K. Nazeeruddin, R. Humphry-Baker, D. L. Officer, W. M. Campbell, A. K. Burrell, M. Grätzel, *Langmuir* **2004**, *20*, 6514–6517.

[70] W. M. Campbell, A. K. Burrell, D. L. Officer, K. W. Jolley, *Coord. Chem. Rev.* **2004**, *248*, 1363–1379.

[71] a) J. K. Park, H. R. Lee, J. Chen, H. Shinokubo, A. Osuka, D. Kim, *J. Phys. Chem. C* **2008**, *112*, 16691–16699; b) A. J. Mozer, P. Wagner, D. L. Officer, G. G. Wallace, W. M. Campbell, M. Miyashita, K. Sunahara, S. Mori, *Chem. Commun.* **2008**, 4741–4743.

[72] a) T. Ma, K. Inoue, K. Yao, H. Noma, T. Shuji, E. Abe, J. Yu, X. Wang, B. Zhang, *J. Electroanal. Chem.* **2002**, *537*, 31–38; b) J. N. Clifford, G. Yahioglu, L. R. Milgrom, J. R. Durrant, *Chem. Commun.* **2002**, 1260–1261; c) T. Ma, K. Inoue, H. Noma, K. Yao, E. Abe, *J. Photochem. Photobiol. A: Chem.* **2002**, *152*, 207–212; d) F. Odobel, E. Blart, M. Lagrée, M. Villieras, H. Boujtita, N. E. Murr, S. Caramori, C. A. Bignozzi, *J. Mater. Chem.* **2003**, *13*, 502–510; e) S. Eu, S. Hayashi, T. Umeyama, A. Oguro, M. Kawasaki, N. Kadota, Y. Matano, H. Imahori, *J. Phys. Chem. C* **2007**, *111*, 3528–3537; f) J. Rochford, D. Chu, A. Hagfeldt, E. Galoppini, *J. Am. Chem. Soc.* **2007**, *129*, 4655–4665; g) A. J. Morris, A. Marton, G. J. Meyer, *Inorg. Chem.* **2008**, *47*, 7681–7685.

[73] Q. Wang, W. M. Campbell, E. E. Bonfantani, K. W. Jolley, D. L. Officer, P. J. Walsh, K. Gordon, R. Humphry-Baker, M. K. Nazeeruddin, M. Grätzel, *J. Phys. Chem. B* **2005**, *109*, 15397–15409.

[74] W. M. Campbell, K. W. Jolley, P. Wagner, K. Wagner, P. J. Walsh, K. C. Gordon, L. Schmidt-Mende, M. K. Nazeeruddin, Q. Wang, M. Grätzel, D. L. Officer, *J. Phys. Chem. C* **2007**, *111*, 11760–11762.

[75] a) M. Tanaka, S. Hayashi, S. Eu, T. Umeyama, Y. Matano, H. Imahori, *Chem. Commun.* **2007**, 2069–2071; b) S. Hayashi, Y. Matsubara, S. Eu, H. Hayashi, T. Umeyama, Y. Matano, H. Imahori, *Chem. Lett.* **2008**, *37*, 846–847.

[76] S. Eu, S. Hayashi, T. Umeyama, Y. Matano, Y. Araki, H. Imahori, *J. Phys. Chem. C* **2008**, *112*, 4396–4405.

[77] A. C. Khazraji, S. Hotchandani, S. Das, P. V. Kamat, *J. Phys. Chem. B* **1999**, *103*, 4693–4700.

[78] a) K. Sayama, K. Hara, N. Mori, M. Satsuki, S. Suga, S. Tsukagoshi, Y. Abe, H. Sugihara, H. Arakawa, *Chem. Commun.* **2000**, 1173–1174; b) K. Sayama, S. Tsukagoshi, K. Hara, Y. Ohga, A. Shinpou, Y. Abe, S. Suga, H. Arakawa, *J. Phys. Chem. B* **2002**, *106*, 1363–1371; c) K. Sayama, S. Tsukagoshi,

T. Mori, K. Hara, Y. Ohga, A. Shinpo, Y. Abe, S. Suga, H. Arakawa, *Sol. Energy Mater. Sol. Cells* **2003**, *80*, 47–71.
[79] a) P. Persson, R. Bergström, S. Lunell, *J. Phys. Chem. B* **2000**, *104*, 10348–10351; b) Y. Wang, K. Hang, N. A. Anderson, T. Lian, *J. Phys. Chem. B* **2003**, *107*, 9434–9440.
[80] E. L. Tae, S. H. Lee, J. K. Lee, S. S. Yoo, E. J. Kang, K. B. Yoon, *J. Phys. Chem. B* **2005**, *109*, 22513–22522.
[81] a) Q. Dai, J. Rabani, *Chem. Commun.* **2001**, 2142–2143; b) Q. Dai, J. Rabani, *New J. Chem.* **2002**, *26*, 421–426; c) Q. Dai, J. Rabani, *J. Photochem. Photobiol. A: Chem.* **2002**, *148*, 17–24; d) R. Mosurkal, J.-A. He, K. Yang, L. A. Samuelson, J. Kumar, *J. Photochem. Photobiol. A: Chem.* **2004**, *168*, 191–196; e) T. Matsubara, Y. Ichikawa, K. Aramaki, A. Katagiri, *Sol. Energy Mater. Sol. Cells* **2005**, *85*, 269–275; f) G. R. A. Kumara, S. Kaneko, M. Okuya, B. Onwona-Agyeman, A. Kono, K. Tennakone, *Sol. Energy Mater. Sol. Cells* **2006**, *90*, 1220–1226; g) A. S. Polo, N. Y. M. Iha, *Sol. Energy Mater. Sol. Cells* **2006**, *90*, 1936–1944.
[82] J. S. Hong, M. Joo, R. Vittal, K.-J. Kim, *J. Electrochem. Soc.* **2002**, *149*, E493–E496.
[83] Y. Hao, M. Yang, C. Yu, S. Cai, M. Liu, L. Fan, Y. Li, *Sol. Energy Mater. Sol. Cells* **1998**, *56*, 75–84.
[84] J. K. Mwaura, X. Zhao, H. Jiang, K. S. Schanze, J. R. Reynolds, *Chem. Mater.* **2006**, *18*, 6109–6111.
[85] a) Y.-G. Kim, J. Walker, L. A. Samuelson, J. Kumar, *Nano Lett.* **2003**, *3*, 523–525; b) G. K. R. Senadeera, T. Kitamura, Y. Wada, S. YAnagida, *Sol. Energy Mater. Sol. Cells* **2005**, *88*, 315–322.
[86] Y.-G. Kim, J. Walker, L. A. Samuelson, J. Kumar, *Appl. Phys. Lett.* **2003**, *83*, 5470–5472.
[87] X. Liu, R. Zhu, Y. Zhang, B. Liu, S. Ramakrishna, *Chem. Commun.* **2008**, 3789–3791.
[88] J. Ohshita, J. Matsukawa, M. Hara, A. Kunai, S. Kajiwara, Y. Ooyama, Y. Harima, M. Kakimoto, *Chem. Lett.* **2008**, *37*, 316–317.
[89] Y. Chen, Z. Zeng, C. Li, W. Wang, X. Wang, B. Zhang, *New J. Chem.* **2005**, *29*, 773–776.
[90] C. Li, W. Wang, X. Wang, B. Zhang, Y. Cao, *Chem. Lett.* **2005**, *34*, 554–555.
[91] S. Tatay, S. A. Haque, B. O'Regan, J. R. Durrant, W. J. H. Verhees, J. M. Kroon, A. Vidal-Ferran, P. Gaviña, E. Palomares, *J. Mater. Chem.* **2007**, *17*, 3037–3044.
[92] a) A. Burke, L. Schmidt-Mende, S. Ito, M. Grätzel, *Chem. Commun.* **2007**, 234–236; b) A. Burke, S. Ito, H. Snaith, U. Bach, J. Kwiatkowski, M. Grätzel, *Nano Lett.* **2008**, *8*, 977–981.
[93] S. Alex, U. Santhosh, S. Das, *J. Photochem. Photobiol. A: Chem.* **2005**, *172*, 63–71.
[94] J.-H. Yum, P. Walter, S. Huber, S. Rentsch, T. Geiger, F. Nüesch, F. D. Angelis, M. Grätzel, M. K. Nazeeruddin, *J. Am. Chem. Soc.* **2007**, *129*, 10320–10321.
[95] a) A. Ehret, L. Stuhl, M. T. Spitler, *Electrochim. Acta* **2000**, *45*, 4553–4557; b) A. Ehret, L. Stuhl, M. T. Spitler, *J. Phys. Chem. B* **2001**, *105*, 9960–9965; c) K. Takechi, P. K. Sudeep, P. V. Kamat, *J. Phys. Chem. B* **2006**, *110*, 16169–16173.
[96] K. Sayama, K. Hara, Y. Ohga, A. Shinpou, S. Suga, H. Arakawa, *New J. Chem.* **2001**, *25*, 200–2002.
[97] a) M. Guo, P. Diao, Y.-J. Ren, F. Meng, H. Tian, S.-M. Cai, *Sol. Energy Mater. Sol. Cells* **2005**, *88*, 23–35; b) X. Chen, J. Guo, X. Peng, M. Guo, Y. Xu, L. Shi, C. Liang, L. Wang, Y. Gao, S. Sun, S. Cai, *J. Photochem. Photobiol. A: Chem.* **2005**, *171*, 231–236.
[98] a) W.-H. Zhan, W.-J. Wu, J.-L. Hua, Y.-H. Jing, F.-S. Meng, H. Tian, *Tetrahedron Lett.* **2007**, *48*, 2461–2465; b) X. Ma, J. Hua, W. Wu, Y. Jin, F. Meng, H. Tian, *Tetrahedron* **2008**, *64*, 345–350; c) W. Wu, J. Hua, Y. Jin, W. Zhan, H. Tian, *Photochem. Photobiol. Sci.* **2008**, *7*, 63–68.
[99] a) J. He, A. Hagfeldt, S.-E. Lindquist, H. Grennberg, F. Korodi, L. Sun, B. Åkermark, *Langmuir* **2001**, *17*, 2743–2747; b) V. Aranyos, J. Hjelm, A. Hagfeldt, H. Grennberg, *J. Porphyrins Phthalocyanines* **2001**, *5*, 609–616.
[100] M. D. Nazeeruddin, R. Humphry-Baker, M. Grätzel, D. Wöhrle, G. Schnurpfeil, G. Schneider, A. Hirth, N. Trombach, *J. Porphyrins Phthalocyanines* **1999**, *3*, 230–237.
[101] J. He, G. Benkö, F. Korodi, T. Polivka, R. Lomoth, B. Åkermark, L. Sun, A. Hagfeldt, V. Sundström, *J. Am. Chem. Soc.* **2002**, *124*, 4922–4932.
[102] a) P. Y. Reddy, L. Giribabu, C. Lyness, H. J. Snaith, C. Vijaykumar, M. Chandrasekharam, M. Lakshmikantam, J.-H. Yum, K. Kalyanasundaram, M. Grätzel, M. K. Nazeeruddin, *Angew. Chem. Int. Ed.* **2007**, *46*, 373–376; b) L. Giribabu, C. V. Kumar, V. G. Reddy, P. Y. Reddy, C. S. Rao, S.-R. Jang, J.-H. Yum, M. D. Nazeeruddin, M. Grätzel, *Sol. Energy Mater. Sol. Cells* **2007**, *91*, 1611–1617.
[103] a) J.-J. Cid, J.-H. Yum, S.-R. Jang, M. K. Nazeeruddin, E. Martinez-Ferrero, E. Palomares, J. Ko, M. Grätzel, T. Torres, *Angew. Chem. Int. Ed.* **2007**, *46*, 8358–8362; b) J.-H. Yum, S.-R. Jang, R. Humphry-Baker, M. Grätzel, J.-J. Cid, T. Torres, M. D. NAzeeruddin, *Langmuir* **2008**, *24*, 5636–5640.
[104] a) E. Palomares, M. V. Martinez-Diaz, S. A. Haque, T. Torres, J. R. Durrant, *Chem. Commun.* **2004**, 2112–2113; b) A. Morandeira, I. López-Duarte, M. V. Martinez-Diaz, B. O'Regan, C. Shuttle, N. A. Haji-Zainulabidin, T. Torres, E. Palomares, J. R. Durrant, *J. Am. Chem. Soc.* **2007**, *129*, 9250–9251; c) B. C. O'Regan, I. López-Duarte, M. V. Martinez-Diaz, A. Forneli, J. Albero, A. Morandeira, E. Palomares, T. Torres, J. R. Durrant, *J. Am. Chem. Soc.* **2008**, *130*, 2906–29071.
[105] S. Eu, T. Katoh, T. Umeyama, Y. Matano, H. Imahori, *Dalton Trans.* **2008**, 5476–5483.
[106] a) G. Wittig, U. Schöllkopf, *Chem. Ber.* **1954**, *87*, 1318–1330; b) P. J. Murphy, S. E. Lee, *J. Chem. Soc. Perkin Trans. 1* **1999**, 3049–3066.
[107] a) A. Vilsmeier, A. Haack, *Ber. Dtsch. Chem. Ges.* **1927**, *60*, 119–122; b) M. M. Ali, Tasneem, K. C. Rajanna, P. K. S. Prakash, *Synlett* **2001**, 251–253.
[108] a) E. Knoevenagel, *Ber. Dtsch. Chem. Ges.* **1898**, *31*, 2596–2619; b) E. Angeletti, C. Canepa, G. Martinetti, P. Venturello, *J. Chem. Soc. Perkin Trans. 1* **1989**, 105–107; c) P. Kim, M. M. Olmstead, M. H. Nantz, M. Kurth, *Tetrahedron Lett.* **2000**, *41*, 4029–4032.
[109] a) N. Miyaura, A. Suzuki, *Chem. Rev.* **1995**, *95*, 2457–2483; b) S. P. Stanforth, *Tetrahedron* **1998**, *54*, 263–303; c) C. R. LeBlond, A. T. Andrews, Y. Sun, J. R. Sowa Jr., *Org. Lett.* **2001**, *3*, 1555–1557.
[110] a) J. F. Hartwig, *Acc. Chem. Res.* **1998**, *31*, 852–860; b) J. F. Hartwig, M. Kawatsura, S. I. Hauck, K. H. Shaughnessy, L. M. Alcazar-Roman, *J. Org. Chem.* **1999**, *64*, 5575–5580.
[111] a) D. Milstein, J. K. Stille, *J. Am. Chem. Soc.* **1978**, *100*, 3636–3638; b) D. Milstein, J. K. Stille, *J. Am. Chem. Soc.* **1979**, *101*, 4992–4998; c) H. Nakamura, M. Bao, Y. Yamamoto, *Angew. Chem. Int. Ed.* **2001**, *40*, 3208–3210.
[112] J. R. Lenhard, B. R. Hein, *J. Phys. Chem.* **1996**, *100*, 17287–17296.

Received: March 5, 2009
Published Online: April 30, 2009

